REGIME MAP DEVELOPMENT FOR CO-ROTATING TWIN SCREW GRANULATION

by

WEI-DA TU

A thesis submitted to The University of Birmingham for the degree of MASTER OF PHILOSOPHY

Department of Chemical Engineering
School of Engineering
The University of Birmingham
May 2009

Abstract

Continuous granulation is an important process for the future PAT (Processes analytical technology) initiative for the FDA. Therefore it is important to investigate the relationship between operating conditions and the granules. This thesis focused on one of the main equipments – twin screw extruder and attempted to develop the regime maps and the granulation hypothesis for twin screw granulation. In order to compare the mechanism with high-shear granulation that has been studied [1], the same materials were chosen (MCC (Microcrystalline cellulose) 102 and aqueous Polyethylene Glycol (PEG) 6000) and the regime maps were plotted by following similar operating conditions with reference [1]. One regime (granulation behaviour) was recognised for the short mixing geometry (16 mm, 30°), while three regimes (granulation, extrudates and blocked behaviours) were recognised for the long mixing geometry (64 mm, 30°). The regime maps suggested that the optimal granulation (narrow GSD (granule size distribution) and large mean granule size) can be achieved with a higher LS (Liquid-to-solid) ratio and a higher screw speed. The GSD was found further improved by reprocessing the same granules and/or manufacturing with aggressive mixing conditions.

Keywords: twin screw extruder, granulation, high shear granulation, regime map, granule size distribution, GSD

Acknowledgements

I would like to express the great thank to my supervisor – Professor Jonathan Seville for your supervision and encouragement. Maybe you don't know that accepting me as your student two years ago, your decision has dramatically and positively changed my life and the way I see the world! Just like being upgraded on the flight to Puerto Rico, I truly thank you again for upgrading me from inside out! Also, I am so grateful to work with Dr. Andy Ingram. Your delightful supervision (and your great patience as well) does improve my work a lot in every aspect. Except for working, you are more like a full time mentor to me than a co-advisor. It is indeed my great pleasure to work and learn from you! I also want to thank all the colleagues from particle technology group as well as the friends in office 106 and this Department. Thank you for sharing your insights and I will never forget the wonderful time we had! Finally I want to thank my family and my girl friend Pi-Mei for your endless supports. I am proud that you are proud of me.

Content

CHAPTER ONE Introduction 1
1.1 Definition of agglomeration/granulation 1
1.2 Application 1
1.3 Classification of size enlargement processes 3
1.3.1 Growth/tumble agglomeration 4
1.3.2 Coating/Layering 4
1.3.3 Agglomeration using pressure 4
1.3.4 Thermal effects 5
1.3.5 Drop formation 5
CHAPTER TWO Theories and mechanisms 6
2.1 Granulation processes (wet granulation) 6
2.1.1 Overview 6
2.1.2 Macroscopic point of view 11
2.1.3 Microscopic point of view 15
2.2 Agglomeration equipments 19
2.2.1 Batch-wise equipments 19
2.2.2 Semi-continuous equipments 22
2.2.3 Continuous equipments 22
2.2.4 Motives of the thesis 26
CHAPTER THREE Methodology 33
3.1 Equipment 33
3.1.1 Co-rotating twin screw extruder 33
3.1.2 Basic measurements 37
3.2 Materials 40
3.3 Experimental processes 42
CHAPTER FOUR Results and discussion 45
4.1 GSD and the growth regime map 45
4.2 Further analysis of the GSD 48
4.3 The effects of screw speed, LS ratio and binder viscosity on torque 49
4.4 Improving the GSD 53
4.4.1 Looping experiment 53
4.4.2 Long single mixing section 59
4.4.3 Staggered mixing sections 69
CHAPTER FIVE Conclusions and comments 76
CHAPTER SIX Future works 78

List of figures

Fig. 1-1 Classification of size enlargement processes [9] 3
Fig. 1-2 Basic concept for wet granulation [11] 4

Fig. 2-1 Modern granulation process description [12] 6
Fig. 2-2 Different saturation states of liquid-bounded granules [12] 7
Fig. 2-3 The growth regime map proposed by Iveson and Litster in 2001 [18] 11
Fig. 2-4 Schematic drawing of a pair of colliding particles 16
Fig. 2-5 Batch-wise granulation equipments. (a) Typical high-shear mixer granulator [25]; (b) Typical fluidized bed (in the picture: Wurster coater) 21
Fig. 2-6 Glatt multicell GMC 30 [58] 22
Fig. 2-7 Schematic drawing of extrusion 23

Fig. 3-1 HAAKE PolyLab System® 35
Fig. 3-2 Schematic cross section of the co-rotating twin screw extruder 35
Fig. 3-3 The screws and the composing sections 37
Fig. 3-4 Basic measurements for the co-rotating twin screw extruder 39
Fig. 3-5 Size measurement of MCC 102 41
Fig. 3-6 Working matrix for the extruder 43
Fig. 3-7 Working matrix for the high shear mixer granulator [1] 43
Fig. 3-8 Liquid injection ports 44

Fig. 4-1 The growth regime map for the extruder with a short single mixing section. Powder: MCC PH 102, Binder: aqueous PEG 6k 33% 47
Fig. 4-2 The irregular and big shreds 48
Fig. 4-3 Further analysis of the GSD 49
Fig. 4-4 Torque analyses 52
Fig. 4-5 The extrudates 53
Fig. 4-6 Looping experiments 57
Fig. 4-7 The change of the mean granule size and each size frequency 58
Fig. 4-8 The work exerted on the granules with the short single mixing section 59
Fig. 4-9 The growth regime map for the extruder with a long single mixing section. Powder: MCC PH 102, Binder: aqueous PEG 6k 33% 62
Fig. 4-10 Torque measurements with the long single mixing section. PEG 6k 33%, dry powder feed rate: 20 g/min 63
Fig. 4-11 Further analysis of the GSD 64
Fig. 4-12 Looping experiments 67
Fig. 4-13 The change of the mean granule size and each size frequency 68
Fig. 4-14 The work exerted on the granules with a long single mixing section 69
Fig. 4-15 The growth regime map for the extruder with staggered mixing sections. Powder: MCC PH 102, Binder: aqueous PEG 6k 33% 71
Fig. 4-16 Further analysis of the GSD 73
Fig. 4-17 Comparisons between short, long single mixing section and staggered mixing section 75

Fig. 6-1 The Freezing method 79

List of tables

Table 2-1 Estimates of Uc for different granulation processes [21]..... 10
Table 2-2 A list of granule property measurements with twin screw extruders and the comments..... 28

CHAPTER ONE

INTRODUCTION

1.1 Definition of agglomeration/granulation

Agglomeration/granulation is a process in which small particles are combined and become a larger entity whilst the individual and primary particles are still distinguishable [2]. The process can be achieved by either dry or wet methods. Liquid materials are used as a linking substance between the particles in wet agglomeration/granulation (usually in a high shear mixer), while dry agglomeration/granulation can be used to produce larger granules through heat treatment (sintering), pressurisation (compaction and extrusion) or by utilizing the cohesive characteristics of the material (tumbling and fluidizing). Agglomeration and granulation are used interchangeably for the same meaning across this thesis.

1.2 Applications

The application of granulation technique is commonly seen in nature, for example the birds' nests are made of mud (solid) and bird's saliva (binder). In industry, it is also a fundamental and widely adopted process ranging from pharmaceutical and food (e.g. cereal bar, cubed bouillon) manufacture, mining and manufacture of agriculture products (e.g. fertilizer). By using specific well-designed techniques, material characteristics can be modified to help produce more easily handled materials. Some advantages that granulation provides are listed below:

- **Product design:**

With a proper granulation technique, the granule properties such as surface area, hardness, bulk density, morphology, size distribution etc. can be modified, achieving a more accurate manufacturing. It is especially very critical for improving modern treatments as the dissolution characteristics of medicines, delivery rates or even taste could be controlled.

- **Reducing dustiness:**

Dustiness could cause waste of materials, dust explosion [3] or even a major threat to the operators who expose themselves to the dusty air. Despite of the filtration techniques, this problem can be reduced by incorporating the dust into larger particles.

- **Flow properties improvement:**

Fine particles are easily affected by high moisture as well as having high Van der Waal's forces; therefore stagnant flowing zones might be formed in some circumstances. It can be avoided by using granulation techniques where particulate materials are "designed" in terms of shape, surface roughness, average size and density. Furthermore, narrower granule size distribution (GSD) can result in less segregation too. For instance, when two or more different size ingredients are mixed, agglomeration can prevent the mixture from segregating and achieve a uniform material distribution.

- **Soil remediation**

In the soil remediation industry, some patterns (Aglofloat® and Aglotherm® technology) based on this technology has also been used to clean up coal fines in the

products [4-6]. Chemicals are added into tailing ponds where the particles settle out of the water, to absorb the mineral matter that had been mined together with coal from coal carbons.

1.3 Classification of size enlargement processes

There are several granulation techniques are available, and can be divided by its processing process and operating environment [7,8]. For instance, in 2007, Jacob [9] summarized the techniques in the system shown in **Fig. 1-1**:

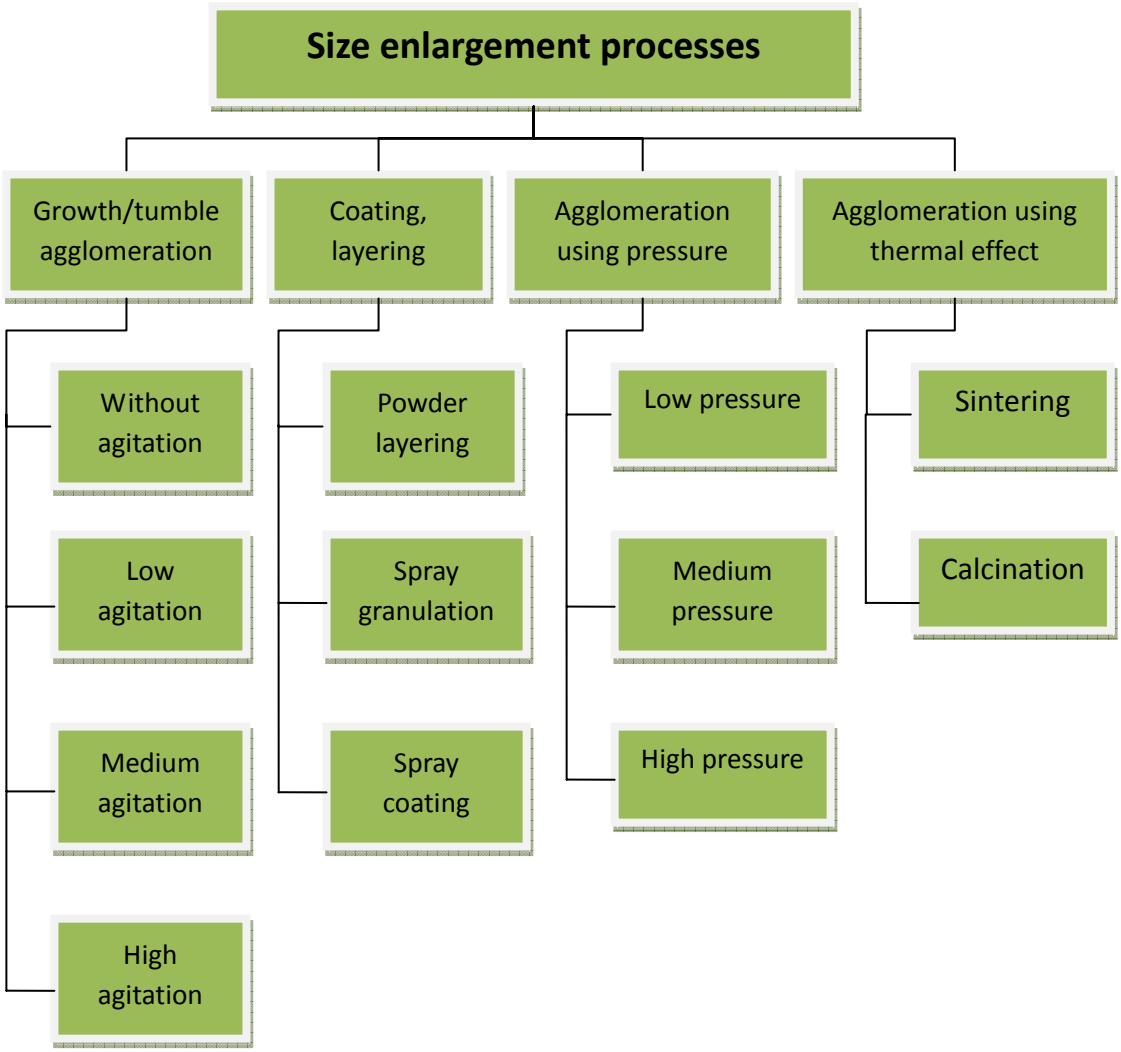

Fig. 1-1 Classification of size enlargement processes [9]

1.3.1 Growth/tumble agglomeration

As shown in **Fig. 1-2** [10], wet granulation is a process in which small primary particles are brought together and combined with each other by adding certain amount of liquid agents and then becomes larger entities gradually. In some cases where continuous agitation is applied, the granule structure can be either staying constant, consolidated or being broken, depending on the magnitude of external impact force, e.g. rotating drum is used to provide low shear forces while high shear mixer granulation features the high shear forces.

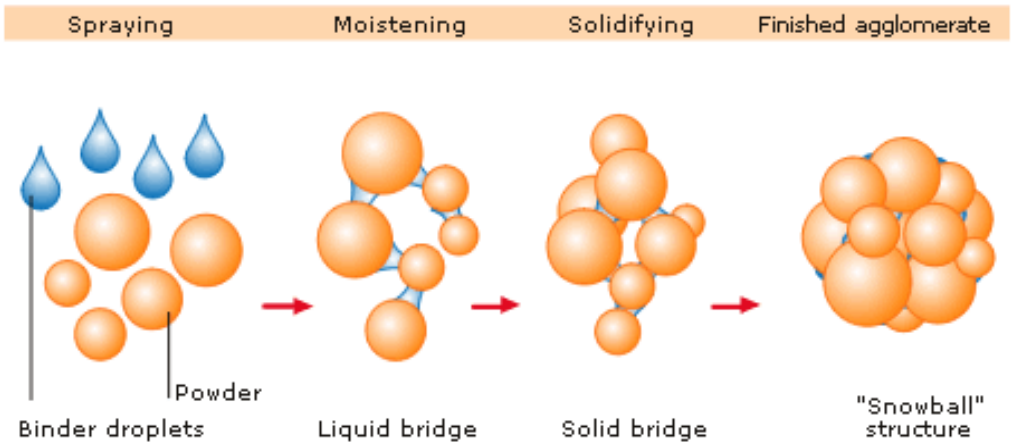

Fig. 1-2 Basic concept for wet granulation [10]

1.3.2 Coating/Layering

This technique is usually seen in rotating drums or coaters (Wurster coater, fluidised bed). While the materials are mixed during the rotation or suspension process, hot air or a liquid spray enters the vessel and covers the particulate raw material. Liquid film will be formed and then it will be dried out by subsequent processes to leave a solid layer on the surface of the raw materials.

1.3.3 Agglomeration using pressure

This technique, including compaction and extrusion is performed via a mechanical

pressurizing process to squeeze particles together. The particles bind to each other by mechanical forces (interlocking) or chemical reactions. They can be achieved with bulk powders containing very small amounts and sometimes even no lubricant or binder additions, unless it is necessary to reduce the friction forces between the particle themselves or between the particles and the die walls.

1.3.4 Thermal effects

Sintering and calcination have been extensively used in metal metallurgy or ceramic manufacturing industries. This method is generally based on heating the component to a temperature above the melting point of at least one of the constituting powders, therefore the composing particles (or grains) can be melted and adhere each other.

1.3.5 Drop formation

In addition to the categories above, Sherrington and Oliver [7] identified another technique – drop formation, or "prilling". Prilling is commonly seen in fertilizer industries. It produces granules in a process where liquid is sprayed from the prilling wheel installed at the top of a hot-air circulated channel. The droplet fall vertically down to a conveyer in the bottom of the channel. By which time, the circulating hot air should have dried out the liquid to leave the solidified particles, known as prills.

CHAPTER TWO
THEORIES AND MECHANISMS

2.1 Granulation processes (wet granulation)

2.1.1 Overview

Wet granulation is a very complex process that is usually composed of several competing mechanisms. The modern granulation process description considers it as a process with three main sets [11,12] as shown in **Fig. 2-1**:

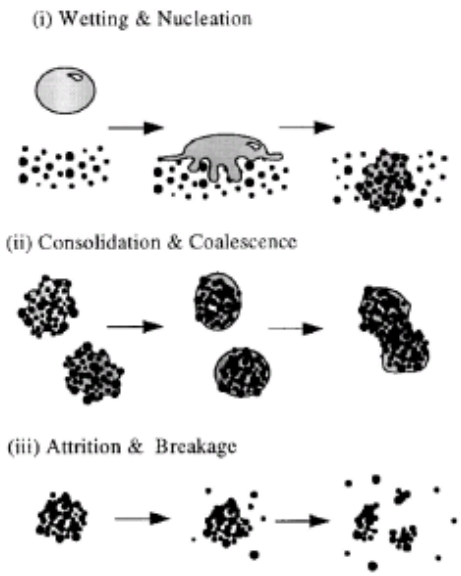

Fig. 2-1 Modern granulation process description [11]

- **Wetting, nucleation and binder dispersion**

This first stage of the process is the contact between the liquid and dry powder. There are two nuclei formation mechanisms [13]: distribution or immersion, depending on the relative size of the droplet to the primary particles. Distribution occurs when binder droplets are smaller than the primary particle and are distributed on the surface of it. These droplet-coated particles are then ready to coalesce. When the particles are far smaller than the droplets, then they will likely to be immersed by the droplets if the surface tension is smaller.

As shown in **Fig. 2-2** [11], it is believed that the liquid existing in the powder bed has five different degrees of saturation state which are the states of pendular, funicular, capillary, pseudo-droplet and droplet [11]. It depends on the granule structure and/or the quantity of liquid contained in the granules. In pendular state, particles are barely connected by liquid bridges. With more liquid addition or more condensed granule structure, funicular and capillary states can occur. When all the particles are held within a droplet without entrapped air, it is called the droplet state or the pseudo-droplet state if air is entrapped.

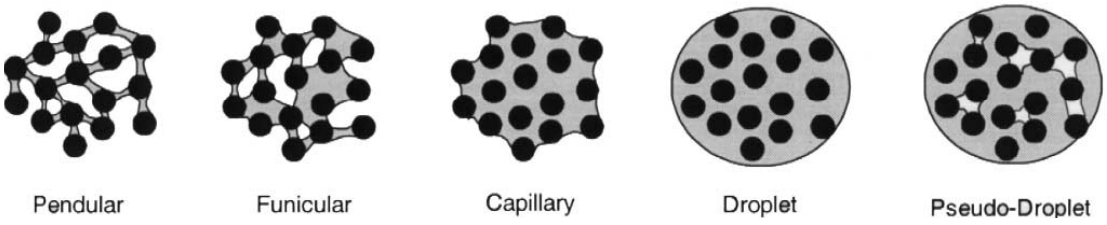

Fig. 2-2 Different saturation states of liquid-bounded granules [11]

It is important to note that the change of saturation state can result in a change of granulation process. For instance, when the primary particles are further impacted, the granule porosity will be decreased and the entrapped liquid and air would be pushed to the surface, thereby the granule could successfully adhere onto other granules, leading to further growth.

- **Consolidation and growth**

When continuous collision between granules takes place, this will reduce the granule size and consequently squeeze the inner liquid and air from the interior to the surface and then form a liquid film. During which, the granule saturation state can be a helpful character for describing this process. In the mean time, granule porosity will be decreased and granules will become more robust due to consolidation. The decrease in granule porosity has been measured and described by an exponential relationship with time that shows a rapid drop at the beginning and then followed by a steady state [14,15]. When the liquid that has been squeezed to the surface becomes thick enough to absorb impact forces from other granules, these granules coalesce and grow.

- **Attrition and breakage**

If the external kinetic energy applied to the granules is higher than a critical value, breakage may occur. The critical value is defined by the Stokes deformation number (St_{def}), which is a ratio of applied energy to the required energy for deformation [16]. This concept is used to help judge whether the granule will be broken by the force exerted by the equipment . St_{def} is defined as eq. (2.1) [17]

$$St_{def} = \frac{\rho_g U_c^{\,2}}{2Y_g} \quad [17] \qquad (2.1)$$

where ρ_g is the granule density, U_c is the representative collision velocity in the

granulator, and Y_g is the dynamic yield stress of the granules.

A relationship between breakage (defined by the breakage number) and St_{def} in high shear mixer has been investigated as shown in eq. (2.2) [18]. The authors dyed a certain size fraction of granules as the tracer particles with erythrosine, and then poured the tracer granules back to the high shear granulator to mix with the tracer-free granules (called the "reference granules" in their work). Afterwards, they measured the total amount of erythrosine present in the size of tracer granules (A_{tracer}) and then divided it with the total amount of erythrosine contained in all the granules (A_{total}). Breakage number was defined as the degree of spread: attrition or breakage.

$$\text{Breakage number} = \left(1 - \frac{A_{tracer}}{A_{total}}\right) \times 100\% \quad [18] \qquad (2.2)$$

where A_{tracer} represents total amount of erythrosine in the tracer granules and A_{total} represents total amount of erythrosine in all the granules. It is noted that the breakage number should be a function of time. The authors [18] plotted the breakage number against St_{def}, and they found a sharp increase in breakage number when St_{def} was at about 0.01, so they defined a border line accordingly between little breakage (attrition) and large extent of breakage.

This approach, however, left a number of questions such as whether breakage was predominately due to high impact forces or the shear in the powder bed because the effects of impact and shear cannot be separated [8]. The estimation of granule velocity in equipment is very critical for calculating St_{def}. Many disagreements about critical St_{def} have been found probably due to disagreement in the estimation of granule velocity. For example, St_{def} = 0.04 was claimed by Iveson *et al.* [17] while St_{def} = 0.2

was claimed by Tardos *et al.* [16]. It is true of course that estimation of granule strength can be inaccurate as well.

In high-shear mixer granulators, Knight *et al.* [19] suggested that U_c could be approximately 20% of the impeller tip speed. The other estimates of U_c for different type of granulation processes are provided in **Table 2-1** [20].

Table 2-1 Estimates of U_c for different granulation processes [20]

Type of granulator	Average U_c	Maximum U_c
Fluidized beds	$\frac{6U_b a_d}{a_b}$	$\frac{6U_b a_d}{a_b l_b^2}$
Tumbling granulators	$w_{dr} a_d$	$\left(w_{dr} D_{drum}\right)/2$
Mixer granulators	$w_{im} a_d$, $w_c a_d$	$\left(w_{im} D_{im}\right)/2$, $\left(w_c D_c\right)/2$

Nomenclature:

U_b: bubble velocity (m/s)
a_b, a_d: bubble size, particle diameter (m)
l_b: dimensionless bubble spacing, defined as the ratio of bubble space over bubble radius
w_{dr}, w_{im}, w_c: drum rotating speed, impeller speed and chopper speed (rpm)
D_{drum} , D_{im} , D_c: diameter of the drum granulator, impeller and chopper (m)

2.1.2 *Macroscopic point of view*

From the macroscopic point of view, a series of granule growth regime maps, defining growth behaviours based on the change of mean granule size with time, have been proposed since 1998 [17,21-23]. **Fig. 2-3** [17] is a typical regime map which features the maximum saturation state (S_{max}) and the Stokes deformation number (St_{def}) as abscissa and ordinate, respectively.

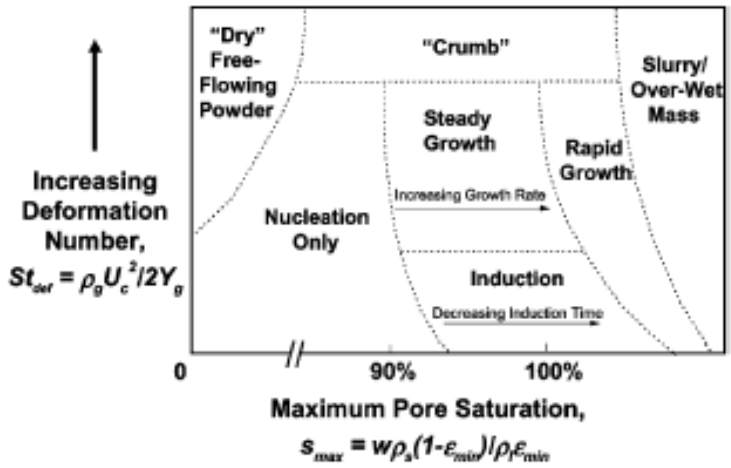

Fig. 2-3 The growth regime map proposed by Iveson and Litster in 2001 [17]

As shown in **Fig. 2-3**, S_{max} is expressed as:

$$S_{\max} = \frac{w\rho_s\left(1-\varepsilon_{\min}\right)}{\rho_l\varepsilon_{\min}} \tag{2.3}$$

where ρ_s and ρ_l are the density of solid particles and the liquid density respectively. w represents the mass ratio of liquid to solid and ε_{min} is the minimum porosity the formulation reaches for that particular set of operating conditions.

A disagreement about the regime map ordinate occurred during the evolution. In 1997, Tardos *et al.* [16] recognised that granule coalescence was a very complicated process since

the amount of binder evaporation is too difficult to predict. They proposed a Stokes' deformation number St_{def} as shown in eq. (2.4 a) with the definition: a ratio of the external applied kinetic energy to the energy required for deformation. It was to simplify the granulation process where $\tau(\dot{\gamma})$ was the characteristic stress. $\tau(\dot{\gamma})$ can be expressed as eq. (2.4 b) (Herschel bulkily equation) where k_{av} is the apparent viscosity and n is the flow index which means the wet granules exhibit both yield strength and non-Newtonian behaviour. By assuming that the granules are composed of extremely concentrated slurry, the apparent viscosity k_{av} can be ignored compared to the yield strength. So that eq. (2.4 b) became eq. (2.4 c). Substitute eq. (2.4 c) into eq. (2.4 a), eq. (2.4 d) can be derived.

$$St_{def} = \frac{\frac{1}{2} m_p U_c^2}{V_p \tau(\dot{\gamma})} \quad [16] \qquad (2.4\text{ a})$$

$$\tau(\dot{\gamma}) = \tau_y + k_{av} \dot{\gamma}^n \quad [16] \qquad (2.4\text{ b})$$

$$\tau(\dot{\gamma}) = \tau_y \quad [16] \qquad (2.4\text{ c})$$

$$St_{def} = \frac{\frac{1}{2} V_p \rho_p U_c^{\,2}}{V_p \tau_y} = \frac{\rho_p U_c^{\,2}}{2\tau_y} \quad [16]$$

However, in 1998, Iveson and Litster [21] suggested that granule deformation could be considered as plastic, so they developed a new number – deformation number (*De*) to quantify the degree of deformation.

$$De = \frac{\rho_g U_c^{\,2}}{Y_g} \quad [21] \qquad (2.5)$$

De is a ratio of applied energy to the plastic energy per unit strain of a granule, and it

describes the deformation with dynamic yield stress instead of τ_y. The disagreement led to ambiguity when drawing the regime maps, until Iveson *et al.* [17] suggested to unify the terminology by replacing τ_y with Y_g in 2001. Finally this integration led to the latest definition of St_{def} as shown below:

$$St_{def} = \frac{\rho_g U_c^{\,2}}{2Y_g} \quad [17] \tag{2.6}$$

The map is a qualitative tool that can explain, understand and sometimes predict growth behaviour under certain operating conditions based on formulation properties before doing experiments or mass production. Therefore saving development cost is considered to be the main advantage of this tool. The map classifies agglomeration behaviour into four categories: nucleation, steady growth, induction and rapid growth. Nucleation occurs when the binder is brought into contact with a powder bed and granule nuclei are formed, but there is not enough binder to promote further growth. Steady growth occurs with weak and deformable granules, resulting in a steady but slow growth. Induction behaviour can be observed in a relatively "stiff" system where the granules are less likely to deform at the beginning. Throughout the entire process of this behaviour, granules will exhibit three stages: (1) they do not deform apparently caused by liquid transformation from inner granules to the surfaces; (2) after which they will grow rapidly due to sufficient coalescence until the third stage; (3) ultimately a steady state for average granules size is reached [14]. Rapid growth could be found when more liquid is added into the system and the induction stage becomes very short.

However, it is noted that the boundaries between behaviours vary with the change of batch, materials, shear force distribution, heat transfer and so on. It is because that the

traditional regime maps, e.g. **Fig. 2-3,** did not aim to define the behaviours with time-dependent characteristics of the granules, e.g. surface stickiness, hardness, deformability, shape, GSD (granule size distribution), force distribution, particle friction forces (internal friction, wall friction) and so on. Relevant researches upon this are still sparse.

For the abscissa of **Fig. 2-3**, ε_{min} was found to be a complex function of formulation properties and operating conditions [17]. It could be estimated in a low intensity granulator, such as a rotating drum, by simply measuring the wet-tapped porosity of the granules because in low intensity granulation, the voidage is closely related to the tapped porosity. On the other hand, in the case of high intensity granulation, e.g. a high shear mixer, it is necessary to do the experimental measurements for prediction. Secondly, the granule saturation state can change if the liquid is evaporated or if the solid dissolves and becomes part of the liquid phase, so that the maximum pore saturation state is employed, instead of granule saturation state [17]. Thirdly, Bouwman *et al.* [24] found that St_{def} was not an appropriate predictive tool in an environment with low viscosity binder (e.g. water) or if the solid can be dissolved and become part of liquid binder. From the same research paper, Bouwman *et al.* [24] defined St_{def} as

$$St_{def} = \frac{\rho_g U_c^{\,2}}{2\sigma_g} \quad [24] \qquad (2.6)$$

where U_c is the representative collision velocity of granules and σ_g is the granule strength. σ_g can be calculated by using the equation (2.7) postulated by Ennis *et at.* [25] who assumed the granules were at a dynamic situation (particles move relative to each other):

$$\sigma_g = \frac{9}{8}\frac{\left(1-\varepsilon_g\right)^2}{\varepsilon_g}\frac{9\mu U_c}{16a_p} \quad [25] \tag{2.7}$$

where ε_g is the granule porosity, μ is the binder viscosity, U_c is the relative collision velocity and a_p is the primary particle size. It can be seen that μ is an important parameter for granule strength and consequently important for St_{def}. Furthermore, Bouwman *et al.* [24] experimentally found that low viscosity binder (such as water) can result in high St_{def}, and can even exceed St_{def}*, the critical value of St_{def}. Therefore the crumb behaviour (disintegration mechanism) will always happen, which is against their tracer experiments. This anomaly was possibly caused by three reasons: (1) In most literature, people have not validated St_{def} with water's viscosity; (2) Even water has been used as the binder, the viscosity is still very high since it dissolves the powder, e.g. lactose; (3) Eq. (2.7) neglects the contribution of the inter-particle friction forces. It might result in a higher Stokes' number, in other words – the crumb behaviour. Therefore in case of a low viscosity binder, they suggested that the easiest way to determine the accompanying granulation regime was to perform a tracer experiment and examine the characteristics of material exchange.

2.1.3 Microscopic point of view

In the microscopic point of view, a dimensionless Stokes' number (*St*) was proposed by Ennis *et al.* [25] to help explain the possibility of coalescence. *St* represents a ratio of initial kinetic energy to the energy dissipated between two colliding particles brought about by interstitial binder which is shown as eq. (2.8) [26] and **Fig. 2-4**.

$$St = \frac{\text{Initial kinetic energy}}{\text{Energy dissipated between two colliding particles}} \tag{2.8}$$

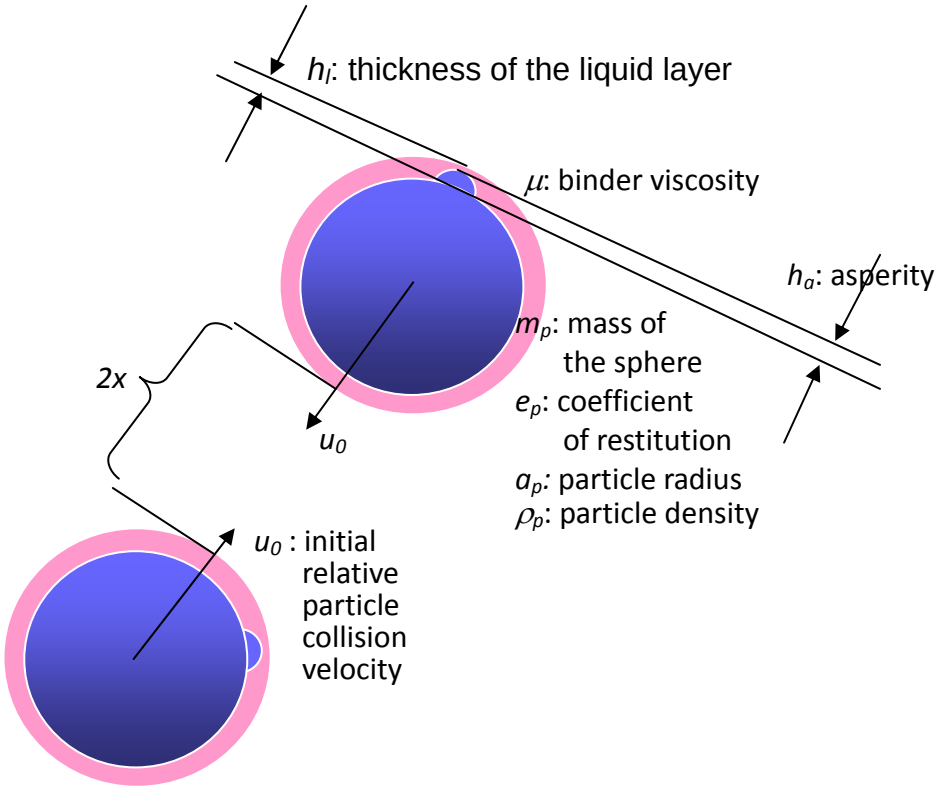

Fig. 2-4 Schematic drawing of a pair of colliding particles

Provided that there is a pair of liquid-covered identical spheres approaching each other along with a line of their centres, a pendular bridge (called dynamic pendular bridge) should form and dissipate the kinetic energy of the colliding particles preventing rebound. Comparing to the liquid bridge formed with a pair of static granules, the one formed in collision situation is called the "dynamic pendular bridge". Ennis *et al.* [25] suggested that an approximate solution for the strength of a dynamic pendular bridge can be expressed as eq. (2.9) which is a superposition of a Laplace-Young capillary pressure F_{cap} acting in the outer contact region and a viscous lubrication pressure F_{vis} acting within the inner contact region, where are shown as eqs. (2.9 b) & (2.9 c). Note that ϕ is the filling angle, C_o is the Laplace-Young pressure deficiency and the Ca is the capillary number. The capillary number is expressed as eq. (2.9 d) where μ is the liquid viscosity, u_0 is the particle velocity and γ is the liquid surface tension.

$$F_{dynamic} = F_{cap} + F_{vis} \quad [25] \tag{2.9 a}$$

$$F_{cap} = \sin^2 \phi (C_0 + 2) \quad [25] \tag{2.9 b}$$

$$F_{vis} = \frac{3Ca}{2\frac{2h}{a_p}} \quad [25] \tag{2.9 c}$$

$$Ca = \frac{\mu u_o}{\gamma} \quad [25] \tag{2.9 d}$$

However, F_{cap} was found no analytical solution in its non-linear form and Ennis *et al.* [25] largely concerned with viscous binders, so they neglected the capillary contribution to the dynamic pendular bridge force and only retained the singular and dominant viscous contribution. This simplification implies that any equation derived from this literature can ONLY apply to the system with viscous binder. Nevertheless, Ennis *et al.* [25] did not clarify the definition of critical viscosity. It causes ambiguity when Bouwman *et al.* [24] attempted to predict the growth behaviours by using Stokes' deformation number St_{def}.

This simplification has been approved experimentally over a full range of capillary numbers [27]. To determine the minimum velocity required for the rebound after collision, Ennis *et al.* [25] considered the force balance between rebound and bridge strength on an individual granule as shown in eq. (2.10 a):

$$m_p \frac{dU_c}{dt} = \pi \mu a_p \left[\frac{3}{2} \frac{Ca}{\frac{2h}{a_p}} \right] \quad [25] \tag{2.10 a}$$

$$U_c = u_0 \left[1 - \frac{1}{St_{vis}} \ln\left(\frac{h_l}{x} \right) \right] \quad [25,28] \tag{2.10 b}$$

$$St_{vis} = \frac{2 m_p u_0}{3 \pi \mu a_p^2} \quad [25] \tag{2.10 c}$$

$$m_p = \frac{4}{3} \pi a_p^3 \rho_p \quad [25] \tag{2.10 d}$$

$$St_{vis} = \frac{8\rho_p u_0 a_p}{9\mu} \quad [25] \qquad (2.10\ e)$$

where m_p is the mass of the particle, U_c is the relative collisional velocity, u_0 is the initial collisional velocity, μ is the binder viscosity, a_p is the particle radius, h_l is the thickness of the liquid layer, ρ_p is the particle density and x in the eq. (2.10 b) is the half of the unknown dimensional gap distance.

Because Ennis *et al.* [25] only took the viscous effects into account, so that eq. (2.9 a) becomes eq. (2.10 a), and this assumption can also lead to an analytic solution of "u_0". Eq. (2.10 b) then can be derived [25,28] by applying the initial condition of $u=u_0$ at $x=h$, where St_{vis} is the viscous Stokes' number shown in eq. (2.10 c). In some particular cases, one can substitute the mass of the particle m_p shown in eq. (2.10 d) into eq. (2.10 c) then we can obtain eq. (2.10 e). In some cases, the subscript of St_{vis} shown in eq. (2.10 e) can be replaced by "coal" meaning that the equation is for describing coalescence [16,29].

In order to rebound after collision, the viscous Stokes' number must exceed its critical value - St_{vis}^*(eq. (2.11)). Let the granule velocity that reaches gap distance h_a (h_a: surface asperity. See **Fig. 2-4**) be u_a, the initial rebound velocity should be eu_a, where e is the restitution coefficient. By applying the initial condition that $u=0$ at $x=h$, eq. (2.11) can be yielded. If $St_{vis} > St_{vis}^*$, particles should rebound after collision. If $St_{vis} < St_{vis}^*$, then coalescence occurs.

$$St_{vis}^* = \left(1+\frac{1}{e}\right)\ln\left(\frac{h_l}{h_a}\right) \quad [25] \qquad (2.11)$$

Remember that the capillary effect neglected in eq. (2.9 a) was feasible in a very

viscous condition. In order to estimate the error caused by this simplification, the critical capillary Stokes' number St_{cap}^{*} given in eq. (2.12) is divided by the critical viscous Stokes' number St_{vis}^{*} shown in eq. (2.11). It can be seen that eq. (2.13) equals zero when $e \rightarrow 1$ and h_l/h_a becomes large. It is to say the capillary effects can be ignored under these conditions. In other words, the particles must be smooth and elastic.

$$St_{cap}^{*} = 2\left(\frac{1}{e^2}-1\right)\left(1-\frac{h_a}{h_l}\right) \quad [25] \tag{2.12}$$

$$\frac{St_{cap}^{*}}{St_{vis}^{*}} = 2\left(\frac{1}{e}-1\right)\frac{\left(1-\frac{h_a}{h_l}\right)}{\ln\left(\frac{h_l}{h_a}\right)} \quad [25] \tag{2.13}$$

These equations (eqs. (2.9) to (2.12)) have become the very basic theories adopted by many researchers nowadays to help explain granule deformation during collisions. For example, if high viscosity binder is added into a system, one could model the granules as surface wet elastic spheres [30] (although it is not always applicable in reality). In this case, the energy absorbed during collision is taken to be the energy absorbed by squeezing interstitial liquid between constitutional particles.

2.2 Agglomeration equipments

2.2.1 Batch-wise equipments

As shown in **Fig. 2-5**, there are two kinds of equipments are designed for batch-wise wet granulation: fluidized beds and high shear mixers. The equipments providing low shear forces, such as fluidized beds have the advantage of better product temperature control. Nevertheless, the high shear force equipments, such as high shear mixers, are usually more popular than the lower ones as it is more likely to disperse very viscous binder efficiently

and lead the final products to a harder structure. At the same time, the high work rate can lead to very high temperature (up to 100˚C), causing damage to the products i.e. thermal decomposition. Also, the binder may become less viscous at high temperature, so that different growth behaviour may be observed as the result of more deformable granules [25]. It is still difficult to determine a theoretical end point of high shear granulation due to complex growth behaviours [31,32]. Yet, both high shear mixers and fluidized beds are batch-wise equipments, generally it is found that inconsistent results sometimes appear when scaling up from laboratorial (up to 15 kg per batch) to industrial size (up to 100 kg per batch) [16,25,33].

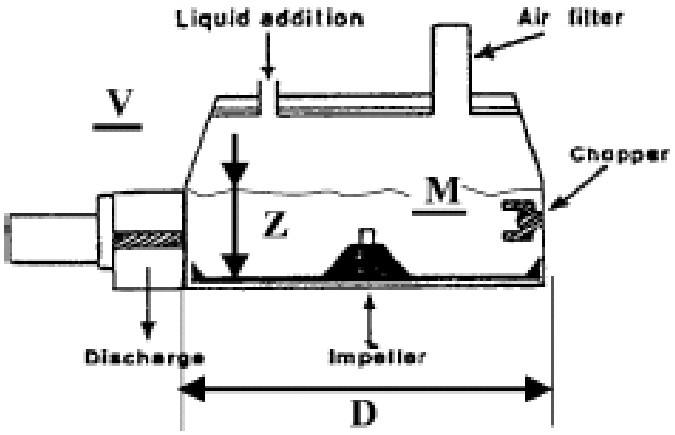

(a) Typical high shear mixer [24]

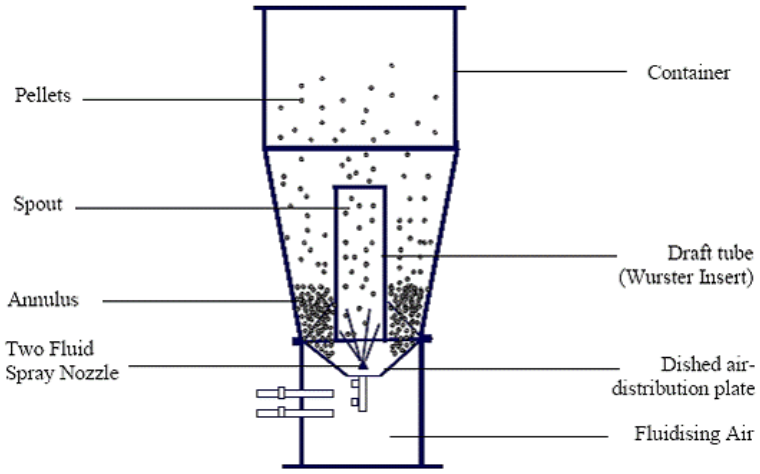

(b) Typical fluidized bed (in the picture: Wurster coater)

Fig. 2-5 Batch-wise granulation equipments. (a) Typical high-shear mixer granulator [24]; (b) Typical fluidized bed (in the picture: Wurster coater)

2.2.2 *Semi-continuous equipments*

Semi-continuous granulation utilizes materials to be processed sequentially from feeding, to mixing and drying. Although the materials are processed continuously, the production line is still a combination of several master batch scale equipments, such as fluidized beds, high shear mixers and/or cyclones, thus the materials are still partly processed in an unsteady state environment. An example is shown below in **Fig. 2-6** [34]:

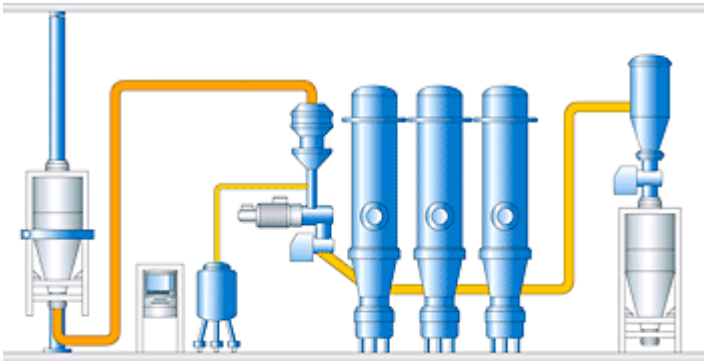

Fig. 2-6 Glatt multicell GMC 30 [34]

The main challenges for such granulation were reported as [35]: (1) the batch size is not well defined, leading to uncertain batch traceability; (2) the system is in general not in the equilibrium state from the beginning.

2.2.3 *Continuous equipments*

Instead of the conventional batch-wise concept for wet granulation, continuous methods have been sought. Single screw extrusion or twin screw extrusion techniques are typical examples.

Extrusion has been a very widely adopted technique in industry (particularly in polymer science related industries) although it is very simple. As a schematic drawing shown in **Fig. 2-7**, a force is applied onto the raw materials filled in the container from one end towards the opposite end. All the materials will then be extruded through a die which defines the final cross section. In practice, the applied force usually comes from one or a pair of rotating screws.

Fig. 2-7 Schematic drawing of extrusion

This technique provides several advantages [36,37]:

1. scale-up problems can be ignored

   Due to the complicated behaviours found in batch-wise wet granulation, and the inconsistent results between different operating scales, the 24/7 manufacturing option – continuous granulation has drawn attention since it can produce many products steadily and efficiently. Therefore, it is not necessary to enlarge the scale in which most inconsistent results may occur. The biggest challenge of this technique, however, is to understand the dominating mechanisms so that the product quality can be controlled.

2. 24/7 automatic production lines would be possible;

3. It can reduce the labour cost.
4. It can reduce the product property variation that might occur in batch-wise equipments.
5. For a twin screw extruder, the screws can self-clean themselves and the equipment as the screws wipe each other [38], leaving only nominal residue after the process.
6. On-line measurement becomes feasible due to the relative simple path of the materials.

This thesis will concentrate on the use of a twin screw extruder. It has been a common and versatile method in food industries [39] and polymer industries. It can be used to obtained uniform products under various inputs. In 1986, Gamlen and Eardley [40] have first introduced the use of a twin extruder - Baker Perkins MP50 to produce paracetamol extrudates. In 1987, Lindberg *et al.* [41] found that the twin screw extruder can be a possible continuous granulation method of pharmaceutical manufacturing with effervescent paracetamol. These researches stated that except for the surface imperfection on extrudates, twin extruder was recommended for making paracetamol granules. Later, Lindberg *et al.* [42] found that granulation via extrusion can yield granules with desired properties under certain operating conditions. Also they found screw configuration can significantly influence the granule porosity. Kleinebudde and Lindner [43] used other materials – lactose and microcrystalline cellulose (MCC) to study the effects of screw speed and water content on the granulation process and extrudates properties.

Recently, the influence of input variables, formulation variables and the granule

characteristics have been further studied [37,44-47]. For the researches mentioned above, different screw speeds and total input rates were usually considered as the input variables. For the formulation variables, different screw profile and die block, binder content and viscosity were usually tested. And for the extrudate/granule characteristics, it was usually of great interest to measure the properties listed in **Table 2-2**. The researches listed above all concluded that a twin screw extruder was an ideal alternative for wet granulation.

The most commonly employed materials for evaluating twin screw granulation are [36,37,44-47]: (1) excipient: α-lactose monohydrate 200M [36,37], microcrystalline cellulose Avicel 101 (MCC 101) [46], sodium guaiazulene sulfonate (GAS-Na) [45] and cornstarch [45]; (2) binder: water [36,37,45,47], demineralized water [44,46], polyethylene glycol (PEG) [44] and aqueous polyvinylpyrrolidone solution (PVP) [36,37,45,47]; (3) model drug (to evaluate the dissolution properties): hydrochlorothiazide (10%) [36,37,47]. It was added to the formulation with and without 2.5% PVP; (4) surfactant [44]: sodium laurylsuphate (SLS), F127 (poloxamer 407), cremophor® RH40 and polysorbate 80.

Although continuous granulation with twin screw extruders is such an efficient method to produce granules, several limitations were found:

1. Extrusion has been an ideal technique for melting and forming polymer into a continuous profile. The axial mixing is probably limited and that means very accurate metering of feed in this technique would be required in the case of blending small quantities of active, which is often seen in the industries of pharmaceutical and chemical manufacturing.
2. The size of container shown in **Fig. 2-7** constrains the size of final products, and that

can be seen more obviously when screws are installed because the path of flowing materials becomes narrower.

3. The processing time for the material in an extruder is much less than that in a high shear mixer, particularly in the case of relative short processing barrel. The output granules may be imperfect in mixing and hardness, due to the lack of work exerted on them. Prolonging the processing time can be achieved by extending the length of barrel or connecting several extruders in series, but both are expensive. Looping processed granules can increase the residence time, but it is not a practical option and will stop the process from being continuous. However, it does not require redesign of the extruder and would be more cost effective for the manufacturers. This thesis will investigate what effects will be caused on the processed granules by using looping method later in Chapter 4.

In fact, most pharmaceutical manufacturers still rely on batch-wise granulation nowadays. Although continuous granulation provides several advantages, its development is still in the early stage therefore the technique is not ready to meet FDA standard.

2.2.4 Motives of the thesis

Agglomeration/granulation has been a critical processing technique in industries and drawn much attention from academics in order to help understand the mechanisms. However, granulation is a very complex process that it is still far from optimal control with the current knowledge. Also, considering that continuous granulation is an important process for the future PAT initiative from the FDA, this thesis aims to further investigate it with various operating parameters (LS (Liquid-to-Solid) ratio, screw speed, viscosity,

processing time, screw configuration). Torque will be measured to help define the relationships between operating parameters, granulation process and the properties of final products.

A work on exploring the regime map for high-shear granulation has been recently developed [1]. This thesis also aims to develop a new growth regime map for an extruder by referring to the working matrix. Comparisons will be made between each other as well. GSD (granule size distribution) will be the main property to represent the rate and extent of material exchange.

Table 2-2 A list of granule property measurements with twin screw extruders and the comments

TESTS	EQUIPMENTS	DESCRIPTION & COMMENTS	EQUATIONS
GSD (Granule size distribution)	• Shaker [48]. • Laser diffraction [36,37].	GSD measurement in these researches was to define the amount of yield, a scale of productivity.	
Yield		It was defined as the mass fraction below 1400 μm [36,37,48]. Unfortunately, the authors did not tell us how much granules are larger than 1400 μm, and it might conceal the real GSD.	
Power consumption and die pressure		They were both monitored during experiments [47]. But in the research work done by Keleb *et al.* [47], this test for them was only to protect the machine if the value was too high.	
Friability	Friabilator (PTF E Pharma Test, Hainburg, Germany) [36,37,48]	Friability is the ability to crumb a solid substance into smaller pieces. It is an important property for storing medicines.	

Morphology		There are many calculations available for defining granule morphology. Generally it tells the appearance of granules, such as a spherical or elongated shape.	• AR (aspect ratio): $AR = \frac{L}{B}$ where L and B were denoted as the length and width of granules. [46] • D_{eq} (equivalent diameter): $D_{eq} = \sqrt{\frac{4 \times A}{\pi}}$ where A represented as the projected area (can be considered as πr^2 if the projected area is a round shape) of the extrudate/granule. [46]
Bulk density (ρ_b)	A normal cylinder.	50 g of extrudates/granules within 250 – 1000 μm were measured in a normal cylinder [36,37].	
Tapped density (ρ_t)	Tapped density measuring device (J. Englesman, Ludwigshafen, Germany) [36,37].	50 g of extrudates/granules within 250 – 1000 μm were measured with 1500 taps (V_{1500}) in a tapping machine [36,37].	
Compressibility index (C)		It is believed that more irregular shape granules can achieve a better compressibility.	$C\ (\%) = \left(\frac{\rho_t - \rho_b}{\rho_t} \right) \times 100$ [36,37], where ρ_t is the tapped density and ρ_b is the bulk density.

Tablet Porosity (ε)	Porosimeters: ● Autopore III mercury porosimeter, (Micromeritics, Norcross, GA, UAS) for pore size distribution [37]. ● He-pycnometry (Micromeritics, Norcross, GA, UAS) for tablet skeletal volume.		$\varepsilon = \left[\frac{(bulk\ \ volume - skeletal\ \ volume)}{(bulk\ \ volume)} \right] \times 100$ [47]
Disintegration time (sec)	It was performed at 37 ˚C: ● with Eur Ph. III (PTZ-E Pharma-Test, Hainburg, Germany) [36,37,47], or with ● VK 7010 (Vankel, Cary, NC, USA) [44]	It is an important product property that tells the medicine absorption rate. One has to note that the conditions of the laboratory test, in vitro, are set to simulate those that occur in vivo.	
Dissolution rate	● Apparatus 1: Vankel, Cray, NC, USA [36,37,47] ● Apparatus 2: USP XXIII [36,37,47]	The test was performed with a paddle method (Vankel, Cray, NC, USA) in a dissolution medium maintained at 37±0.5 ˚C, while the rotation speed was set at 100 rpm (USP XXIII). [36,37,47]	

Stabilization		● Nakamichi *et al.* [45] evaluated the effect of different type of granulator on the stability of Sodium guaiazulene sulfonate (GAS-Na). They found the twin screw extruder was a better choice than the other because its better excipient disperbility can make the granules more stable. ● Stabilization was evaluated by the ratio of remaining GAS-Na to the original content in the final product [45].	
Microscopic image	SEM (Scanning election microscope)	Microscopic images help observing the surface structure of granules produced at different conditions, and the analysis on granule porosity. [37,47]	
Tensile strength (*T*)	● PTB 311 (Pharma Test, Hainburg, Germany) [36,37,47].		$T = \frac{2F}{\pi dt}$, where *F*, *d* and *t* were denoted as the crushing force, product diameter and thickness respectively [36,37,47].

Residence time distribution (RTD)	● Light Meter Type 213 (General Electric, Cleveland, OH, USA) [49] ● COLOR METER IIIF (Minolta, Japan) [49]	When operating an extruder, the mixtures require a certain time to travel through the barrel, called residence time. The concentration of mixture against travelling time forms a distribution curve, called RTD. RTD can help estimate how long does the total material expose to the extrusion processing. Generally, researchers will add tracer dye into raw material and then take digital photos of the extrudates in the downstream. The photos will be digital processed by either Matlab [49] or Photoshop [50]. The colour of extrudates will be transferred into RGB based and converted to device-dependent colour space. Eventually, the change of colour concentration against time (RTD) can be plotted.	*E(t)* and *F(t)* were used to analyze RTD. *E(t)* represents the variation of the concentration of tracer at exit of extruder nozzle with time. *F(t)* represents the cumulative of tracer at the exit with time. C_i represents the concentration at the i^{th} time interval (g/m^3). [49,50] $E(t) = \frac{C}{\int_0^\infty C dt} = \frac{C_i}{\sum_0^\infty C_i \Delta t_i}$ $F(t) = \int_0^\infty E(t) dt = \frac{\sum_0^t C_i \Delta t_i}{\sum_0^\infty C_i \Delta t_i}$ $RTD = \int_0^\infty tE(t) dt = \frac{\sum_0^t t_i C_i \Delta t_i}{\sum_0^\infty C_i \Delta t_i}$

CHAPTER THREE

METHODOLOGY

3.1 Equipment

3.1.1 Co-rotating twin screw extruder

HAAKE PolyLab System PTW 25 (HAAKE®, USA) was employed in this research. The system consists of four main parts as shown in **Fig. 3-1**: The Rheocord torque rheometer, the Rheomex, a powder feeding system and a hydraulic pump:

- **Rheocord torque rheometer – The drive system**
  It provides all functionality for driving and controlling the measuring sensors and feeds back the signals to an external PC. It can be considered as the control centre for the external PC;

- **Rheomex – The Twin Screw Extruder**
  It makes use of two parallel screws which tightly intermesh and which turn in the same rotational direction shown in **Fig. 3-2**. Their circumferential speeds are directed in the opposite directions. The flight of one screw fits tightly into the screw channel of the other and therefore one screw seals mass flow against the other screw.

A general category of the twin screw arrangements can be found in Eise *et al.* [51]. They classified the arrangements by considering (1) the relative rotating directions (co-rotating or counter-rotating), (2) intermeshing (including fully intermeshing and partially intermeshing) or non-intermeshing as well as (3) the engagement of screws (lengthwise and crosswise closed; lengthwise and crosswise open; lengthwise open

and crosswise closed). According to this illustration [51], the type of screws employed in this thesis falls mainly into the category: the fully intermeshing co-rotating twin screw extruder with a lengthwise open and crosswise closed configuration. It is to say the geometry wipe and clean each other, and allow the materials to transfer/exchange in the longitudinal direction.

- **Powder feeding system**

  A feeding hopper is installed above the barrel. It conveys dry and fresh powder constantly to the inlet of the barrel. The feeding hopper is driven by a digital drive controller – Digidrive® which is used to control feeding rate;

- **Hydraulic pump**

  This pump is to steadily deliver liquid for granulation processes. There are three multi-purpose barrel ports located evenly on the top side of the barrel. In this research, liquid was pumped into the barrel through the injection port nearest to the feed port (distance: 11 cm).

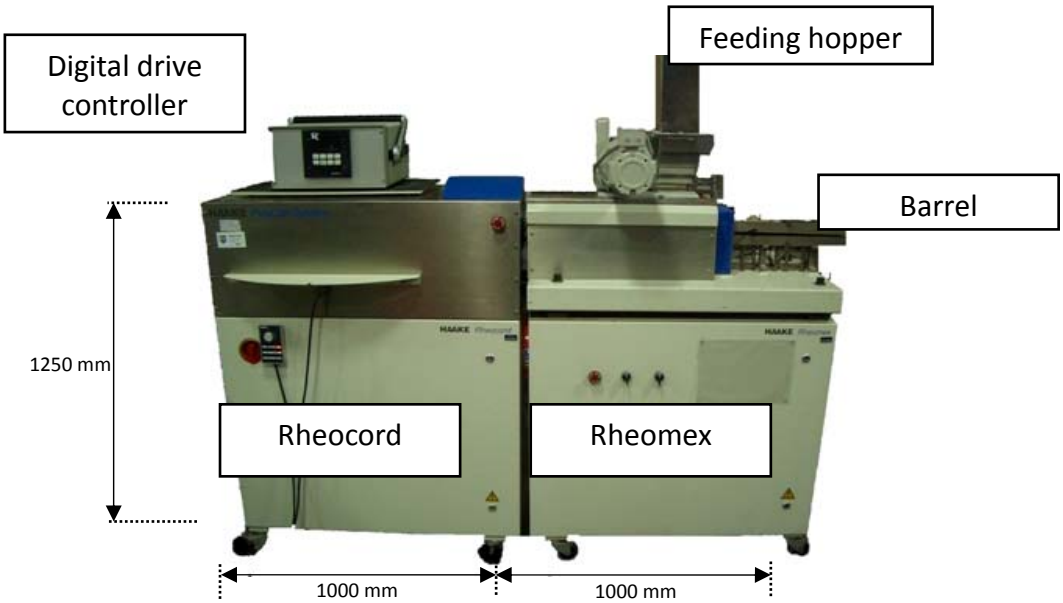

(a) Overview

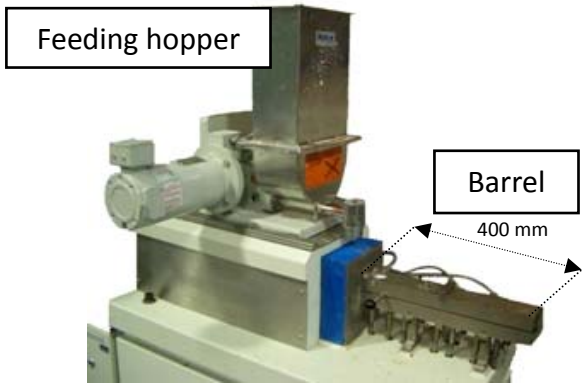

(b) The feeding hopper and the barrel

(c) The hydraulic pump

Fig. 3-1 HAAKE PolyLab System®

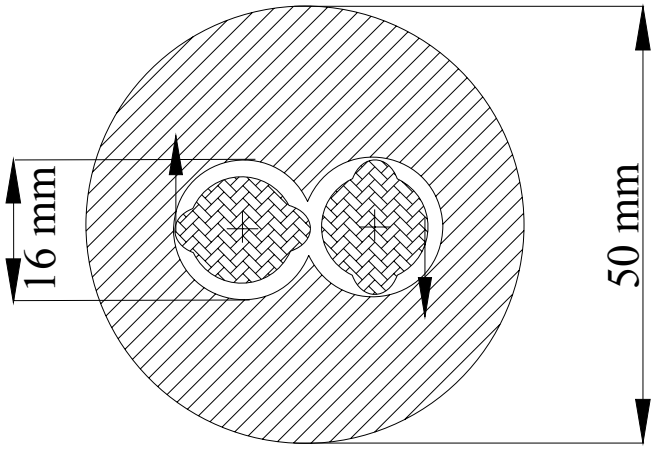

Fig. 3-2 Schematic cross section of the co-rotating twin screw extruder

As shown in **Fig. 3-3**, the two screws are identical and composed of the agitator elements. These agitator elements are made of chromium molybdenum alloy. They can be combined in any order on a screw shaft. The geometry of the screw is defined by L/D ratio, where L means the length of screw and D is the widest diameter of screw. In this research, L/D ratio was 25 (40 cm/1.6 cm). Although there are many possible screw configuration, this thesis, however, considered only few of them because blocking of material may happen as the result of local jamming. It is mainly caused by inappropriate order of the agitator elements so that local pressure of barrel can be too high and harm the machine. **Fig. 3-3** shows one of the screw configuration employed in this research. Each screw consists of four sections which are listed in order: a conveying section, a mixing section (there were four kneading elements staggered with each other with 30°), a conveying section again and the last one – a kneading section. The conveying section or 'feed section' is to transport the raw materials forward. The raw materials will be transported forward and brought into contact with the binding liquid delivering from a hydraulic pump before entering the mixing section. A close-up picture of the mixing section is shown in **Fig. 3-3**. It can be seen that four kneading paddles are placed together and offset at a specific angle. In this picture the offset angle is 30 degrees which is smaller than the conveying section. It means that this mixing section pushes the material forward more slowly than the conveying section; therefore the material will be held here for a longer time and mix with the incoming ones (those from the conveying section). Note that the length of each kneading paddle is 4 mm, forming a 16 mm mixing section. After

mixing, the mixture will then be conveyed forward to the kneading section. Kneading disks can be regarded as elements with 90 degree flight angles, which implies that all flow induced by these elements is in the cross-channel or r direction [52]. Finally the mixture will go through a die block installed in the end of the barrel. Granules can be made by this process under certain operating conditions.

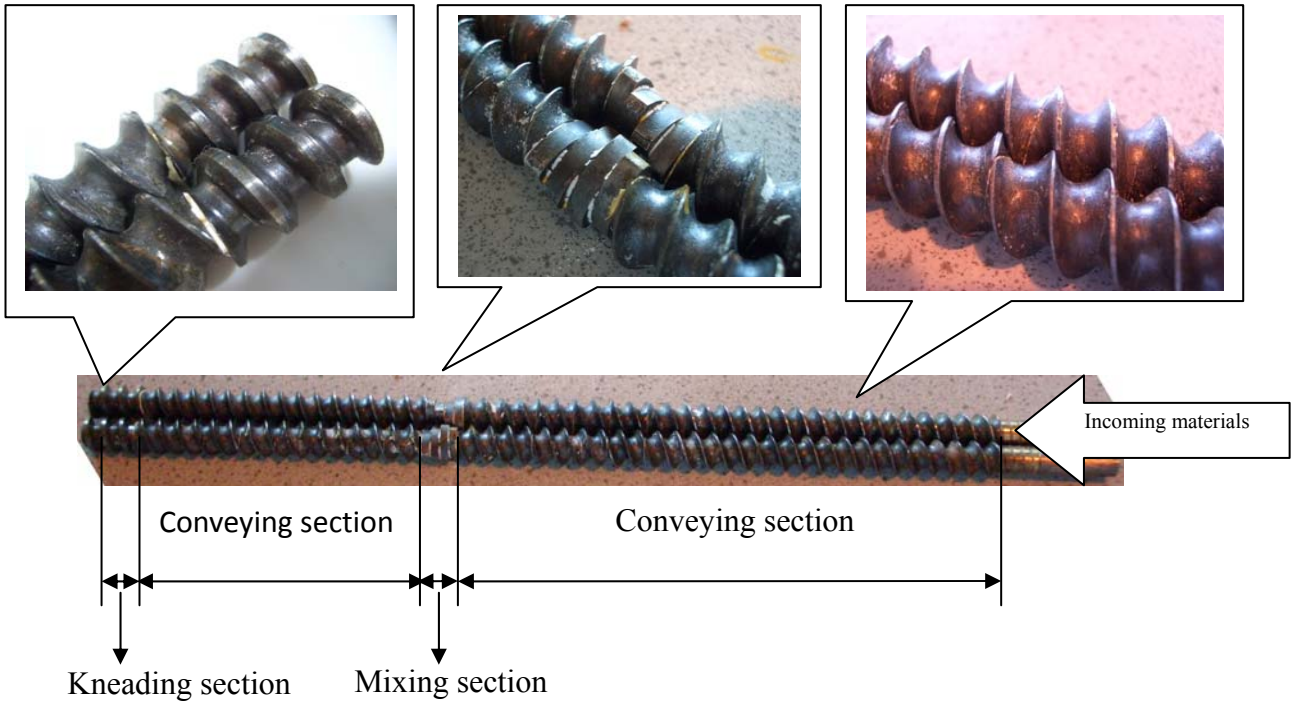

Fig. 3-3 The screws and the composing sections

3.1.2 Basic measurements

In order to determine a proper range of LS ratio for the experiments, firstly it is necessary to measure the mass flow rate of the dry powders and binder. The mass flow rates

for dry powders and binder are shown in **Fig. 3-4 (a)** & **(b)**. Note that dry powder flow rate was measured at ambient humidity 78% and temperature 19.4 ˚C. In addition, as shown in **Fig. 3-4 (c)**, a compatible barrel screw speed must be determined as well to ensure a constant material flow rate throughout experiments, and a consistent flow between the feeding hopper and the barrel. There is an "unworking regime" shown in **Fig. 3-4 (c)**, indicating the barrel screw speed is too slow to carry the feeding powder from the feeding hopper, and it will result in material accumulation in the barrel.

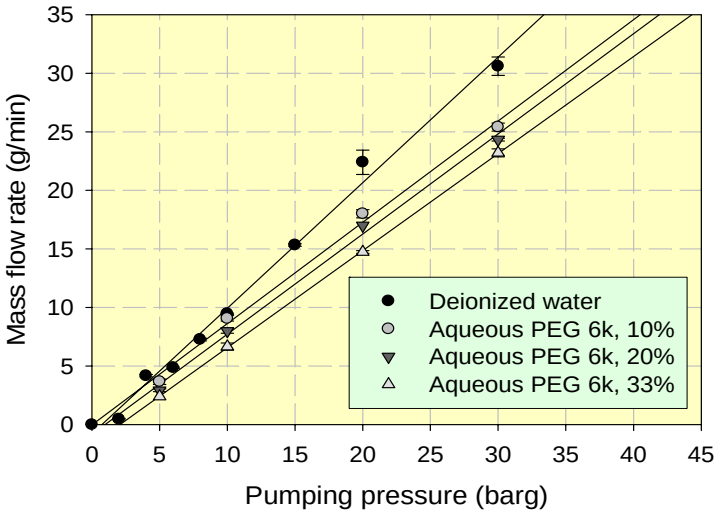

(a) Binder mass flow rate

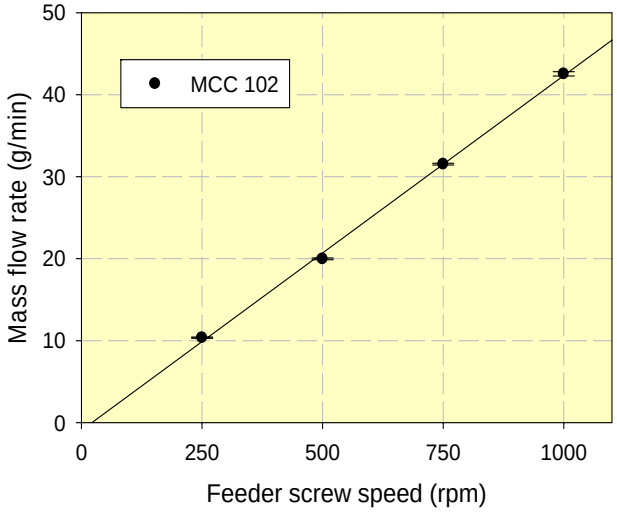

(b) Dry powder mass flow rate (from the feeding hopper)

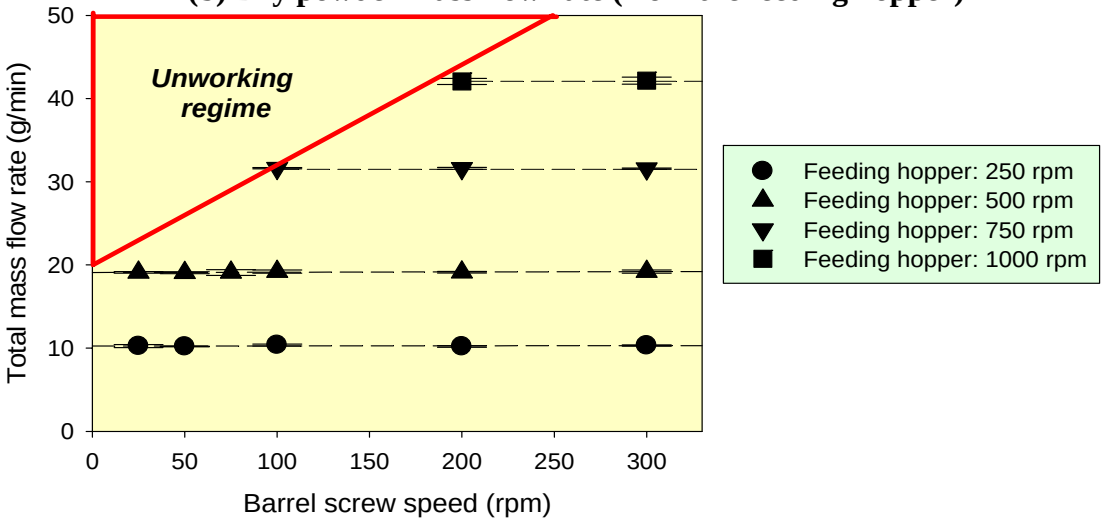

(c) Dry powder mass flow rate (feeding hopper + barrel)

Fig. 3-4 Basic measurements for the co-rotating twin screw extruder

3.2 Materials

3.2.1 Microcrystalline cellulose (MCC) 102

"Cellulose" is a natural product that can be derived from wood pulp and formed into sheets. The individual fibres are then mechanically broken up into small pieces and this process transfers the cellulose into free-flowing powders. However, it is still poor on the fluidity and compressibility until an important modification is applied, which is the isolation of the crystalline part of the cellulose fibre chain. Microcrystalline cellulose (product name: Avicel) is the product made by following this method. There are two most common grades in the market: PH101 and PH102. PH101 is the original product while PH 102 is more agglomerated and larger, resulting in slightly better fluidity but with no significant decrease in compressibility [53].

In this research, MCC Avicel 102 (Microcrystalline Cellulose, Avicel PH 102) was employed, considering its physical properties of being inert and odourless, and unique agglomeration characteristics. It was purchased from FMC BioPolymer (USA). The average particle size was measured by X-ray diffraction technique (Sympatec GmbH, UK) and as shown in **Fig. 3-5** that the d_{50} of MCC 102 was 125.3 μm.

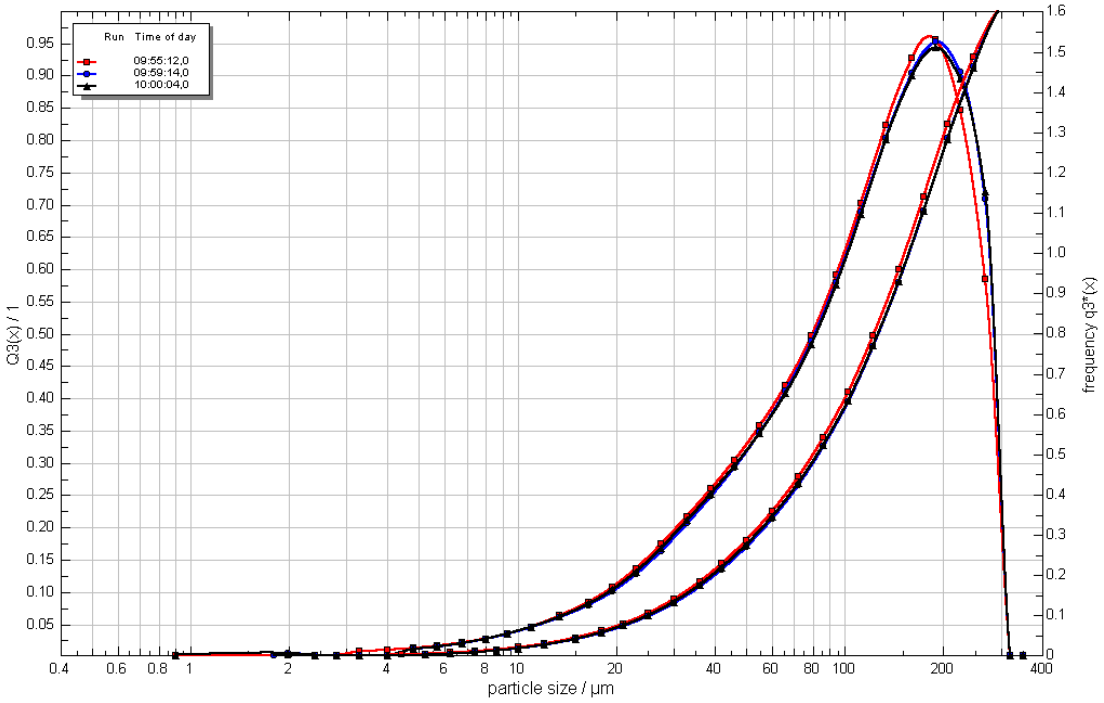

Fig. 3-5 Size measurement of MCC 102

3.2.2 Polyethylene glycol 6000 (PEG 6k)

PEG is available over wide range of products depending on its molecular weight from 300g/mol to 10,000,000 g/mol. The higher the molecular weight is, the higher melting point would be. It is commonly seen in dosage forms because of its low toxicity as well as it can regulate the dissolving time by choosing the molecular weights. In this research, PEG 6k (6000 g/mol), a moderate molecular weight found in literatures, was chosen to be the binder material. It was dissolved in deionized water and the concentration was 33%, making the aqueous solution of PEG 6k. The viscosity was 0.0324 Pas at 25˚C (Advanced rheometer AR 1000, TA instrument).

3.3 Experimental processes

In order to reach a consistent mass flow rate, MCC 102 was firstly conveyed from the feeding hopper through the barrel for 10 minutes, and aqueous PEG 6k 33% was pumped for 10 minutes before connecting to the barrel. Adjust the feeding speeds of the feeding hopper and the barrel respectively to be as consistent as possible, so that material accumulation can be avoided. It is imperative to set the feeding rate of feeding hopper slower than the barrel. Switch on the multi-monitoring program in the control PC, and set the extruder in the manual-control mode. The program is to control and monitor the barrel screw speed, and in the mean time, it can record the real time torque for post analysis.

As shown in **Fig. 3-6**, a working matrix was formed to compare the granulation mechanisms with a high-shear granulation system (seen in **Fig. 3-7** [1]) on the same basis. **Fig. 3-6** featured the same LS ratio with **Fig. 3-7**, but the range was doubled in order to find the border line between solid and slurry regimes. Beside, the agitation speed range in **Fig. 3-6** was lower: 50 rpm, 100 rpm and 200 rpm. This was because granules can be successfully produced within this range.

Connect the hydraulic pump with the barrel and start recording torque. There are three liquid injection ports located evenly on the top side of the barrel as numbered and shown in **Fig. 3-8**. The pump was connected to the first one which was downstream of the dry powder inlet and before the mixing section of the screws.

A dry container facing the barrel outlet will be set up to collect final products. As

long as the final products have been collected, they will be dried out in an oven at 50˚C for 2 hrs before standard sieving procedure. Size distributions were obtained using the assumption that mean granule size on each sieve equalled the arithmetic mean value of the collecting sieve and the one above it.

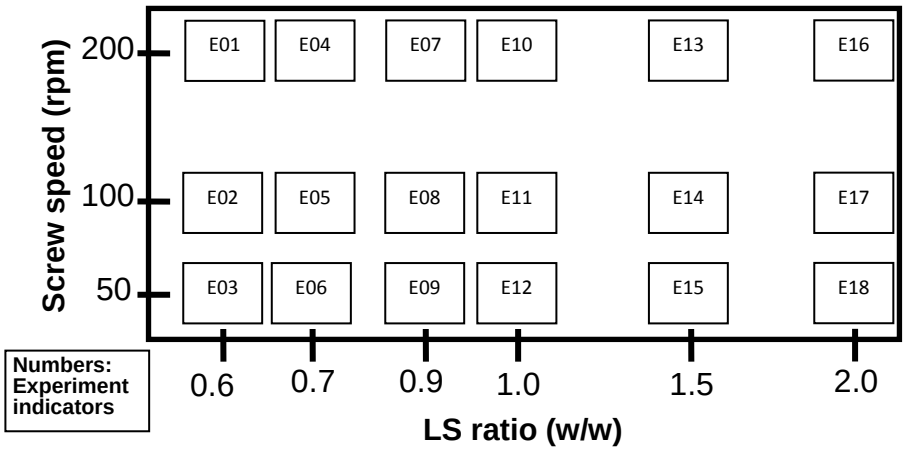

Fig. 3-6 Working matrix for the extruder

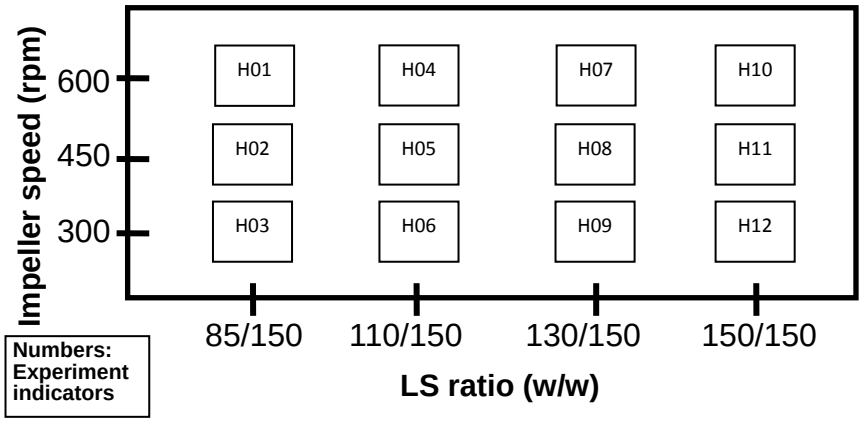

Fig. 3-7 Working matrix for the high shear mixer granulator [1]

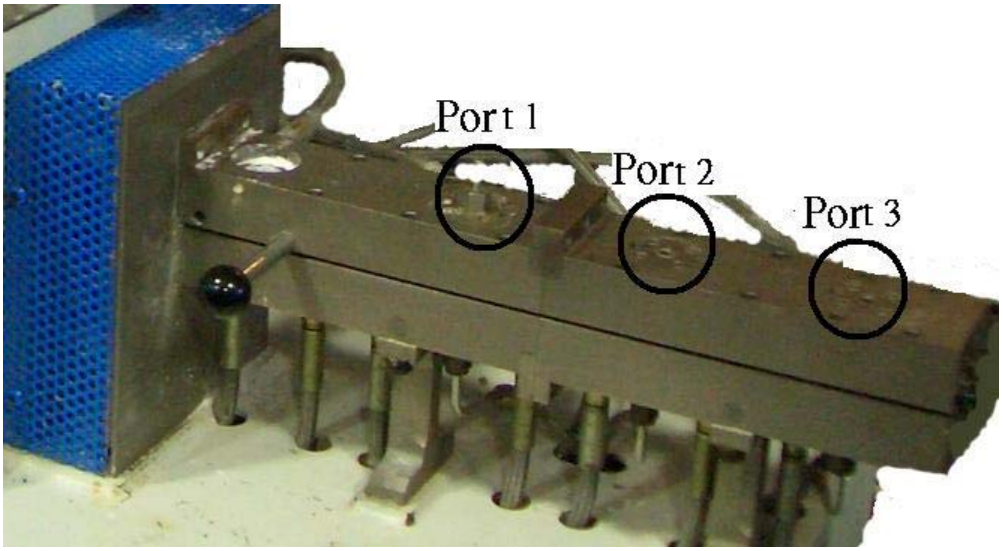

Fig. 3-8 Liquid injection ports

CHAPTER FOUR
RESULTS AND DISCUSSION

4.1 GSD and the growth regime map

By using the geometry of short single mixing section (shown in **Fig. 3-3)**, the GSD of each operating conditions were measured and plotted in **Fig. 4-1** featured with log aperture (μm) in x-axis and mass fraction/delta log aperture (μm^{-1}) in y-axis. Except for the extrudate regime where the system was too wet and the mixture was like paste, the GSD on the rest of the working matrix was found very poor in terms of uniformity. The effect of LS ratio was only obvious at the higher screw speeds (100 and 200 rpm) as these GSD were gradually transferred from bimodal to monomodal from LS = 0.6 to 1.5. Large extent of fines were found in low LS ratio (LS = 0.6 & 0.7) due to lack of binder in the system. For all the operating conditions in **Fig. 4-1**, granules can be produced regardless of the GSD uniformity; therefore the growth regime here was named: granulation.

When the screw speed was at 50 rpm, all the samples contained a lot of "irregular and big" shreds regardless of LS ratio. These shreds are shown in **Fig. 4-2**. The big shreds were deduced to be directly released from the mixing section or kneading section as they looked similar to the screw geometry. Because of the "irregular and big" shreds, the GSD at 50 rpm were found widespread and multi distributed.

While increasing the screw speed, the GSDs were found to be more uniform at higher

LS ratios (LS = 0.9, 1.0 & 1.5). It was presumably because vigorous rotating speed could help narrow the GSD. However, it is still unclear whether the mechanisms are to break up lumps or to promote binder distribution among granules.

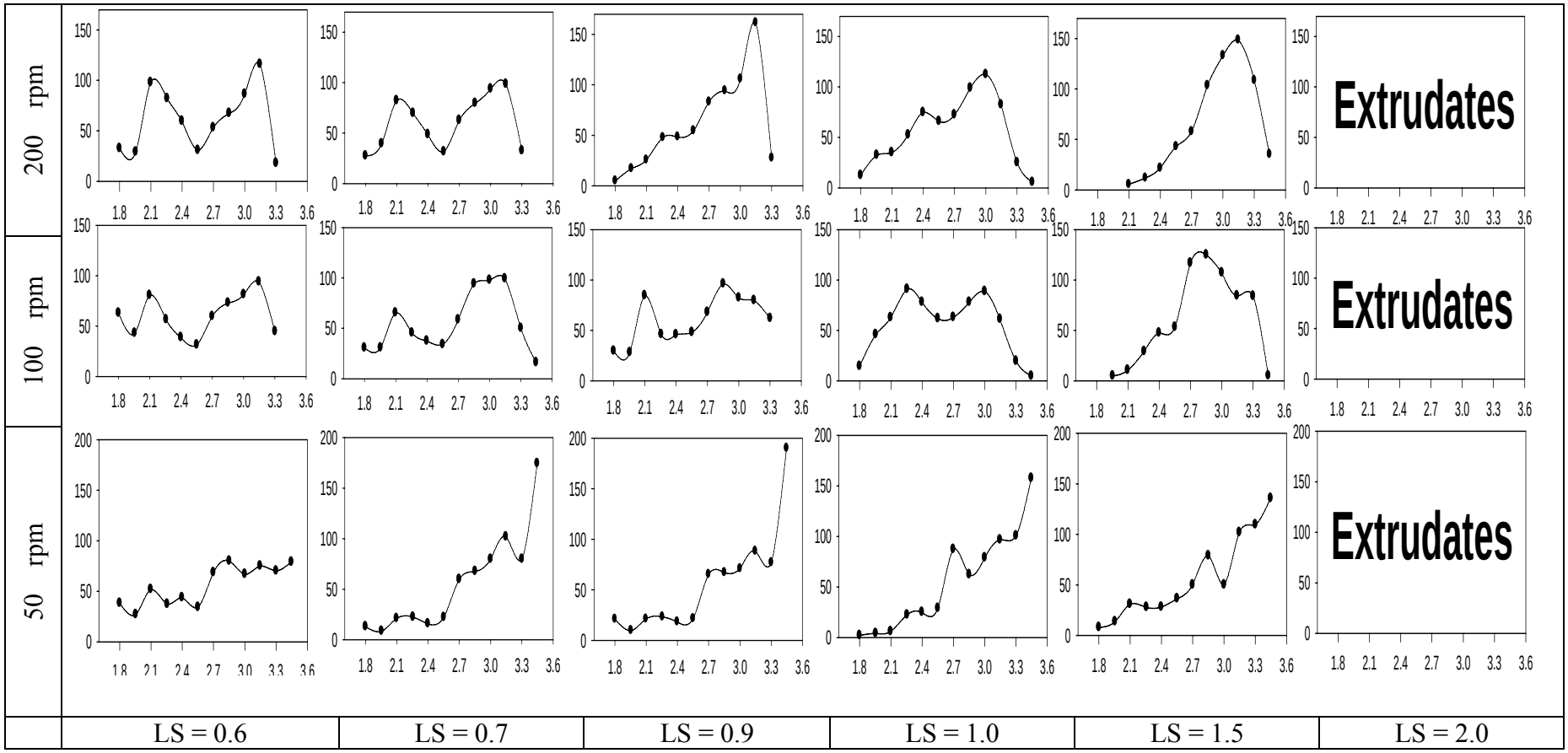

Fig. 4-1 The growth regime map for the extruder with a short single mixing section. Powder: MCC PH 102, Binder: aqueous PEG 6k 33%

Fig. 4-2 The irregular and big shreds

4.2 Further analysis of the GSD

To quantify the GSD uniformity of the granulation regime shown in **Fig. 4-1**, the mean granule sizes and the spread of each distribution curve were plotted in **Fig. 4-3** where the spread was defined as:

$$Spread = \frac{d_{84} - d_{16}}{d_{50}} \tag{4.1}$$

d_{16}, d_{50} and d_{84} represent the mass cumulative frequencies. According to **Fig. 4-3 (a)**, bigger mean granule sizes were found at a low screw speed (50 rpm) regardless of the LS ratio due to the widespread GSD shown in **Fig. 4-3 (b)**. Experiment E13 displayed a big mean granule size with the smallest spread (narrowest GSD), indicating that optimal conditions for a narrow GSD could be achieved with a higher LS ratio and a higher screw speed.

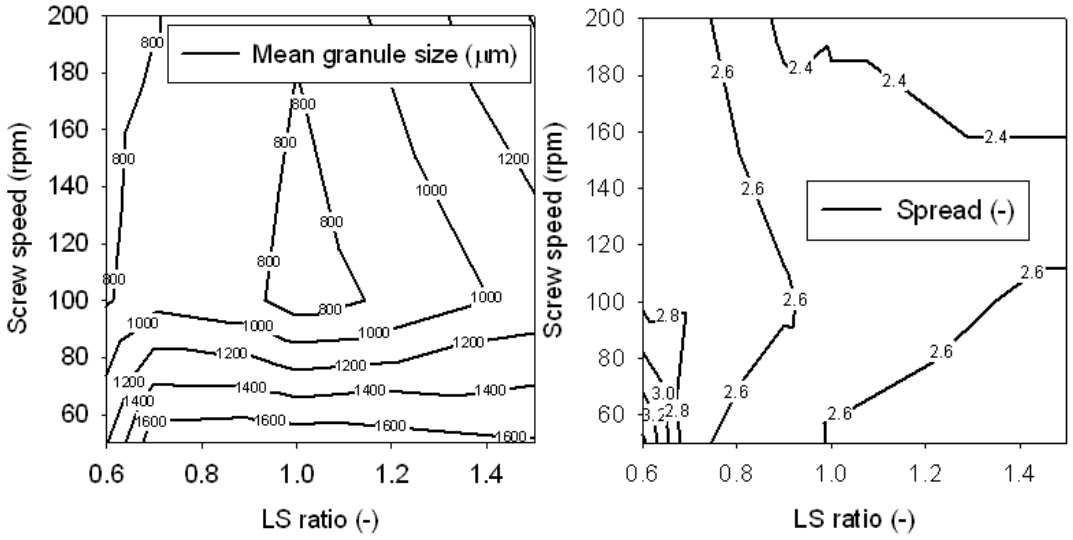

(a) Mean granule size **(b) Spread**

Fig. 4-3 Further analysis of the GSD

4.3 The effects of screw speed, LS ratio and binder viscosity on torque

When either different screw speed and/or LS ratio was applied, it will change the amount of material filled in barrel and the wall friction force (between the mixtures and the inner wall of barrel). Therefore, understanding the effects would be helpful for both the equipment performance and the granulation mechanisms.

Fig. 4-4 (a) was obtained with the dry powder feed rate at 20 g/min. The torque was found a function of LS ratio regardless of the screw speed. With the increase of LS ratio, the torque was kept rising until a critical value (LS = 0.9) and then became lower again. It implies that increasing LS ratio can result in a higher fill level so that it needs more work to rotate the screws. However, in the mean time, **Fig. 4-4 (a)** also shows that the torque decreases again while adding more binder into the system. It implies that either the binder is like lubricant or the binder enhances the flowability of the mixture. Thus it is necessary to investigate the effect of fill level on **Fig. 4-3 (b)** (see later part of Section 4.3).

While the mixture was at LS = 2.0, it seemed that the amount of binder was too much, because the corresponding torque for each rotating screw speed was found very low and very similar regardless of the screw speed, and extrudates (**Fig. 4-5**) can be observed instead of granules. It suggested that a border line distinguishing granules and extrudates (over-wetted state) should locate between LS = 1.5 and 2.0. The twin screw extruder in this study can still produce granules at LS = 1.0 in which the ratio that the uncontrollable growth (granule size increases too quickly to measure and soon exceeds the resolution of sieves) can occur in the high shear mixer. It was probably because the barrel has constrained the size of granules so that the granule size will never go uncontrollably large.

In order to find out the effect of fill level and the relationship between fill level, screw speed and LS ratio, half amount of feeding materials (the dry powder & the binder) was reduced. The corresponding torque was shown in **Fig. 4-4 (b)**. It can be observed that all the torque become very low and they are independent of different LS ratio. According to **Fig. 3-4 (b)**, higher screw speed is supposed to convey more materials in the same time. But the torque in **Fig. 4-4 (b)** shows no significant difference between each screw speed. Therefore, in general, the effect of fill level caused by screw speed can be only seen obvious when it reaches a critical value, where contact force (friction force) can take place between the materials and the inner wall of barrel. Besides, the effect of LS ratio on torque is dependent on the fill level caused by different screw speeds.

Except for the effects of fill level, the effect of binder viscosity was also studied by using a less viscous binder – deionized water. As shown in **Fig. 4-4 (c)**, the amount of

feeding materials was kept the same with **Fig. 4-4 (a)**, but it can be seen that the torque becomes lower. Since the fill level remains the same with **Fig. 4-4 (a)** except for different mixture rheology, it is reasonable to assume the low torque was mainly caused by the addition of water, a binder that is less viscous than aqueous PEG 6k. In fact, the mixture rheology is very complicated. It can be affected by applied stress, working temperature and so on. It is necessary to investigate the relationship of mixture properties and torque in the future.

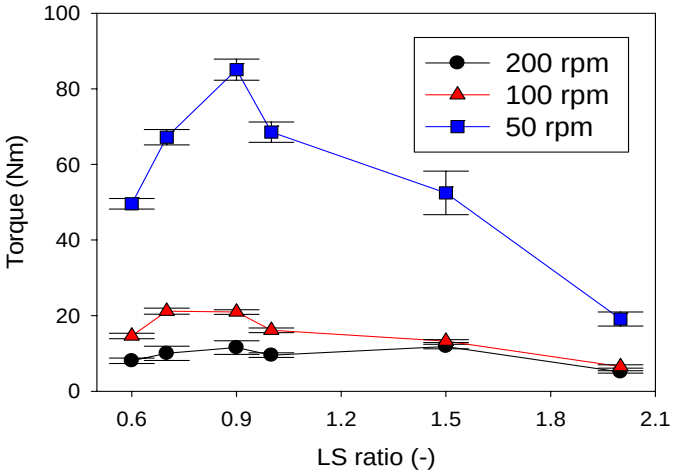

(a) PEG 6k 33%, dry powder feed rate: 20 g/min

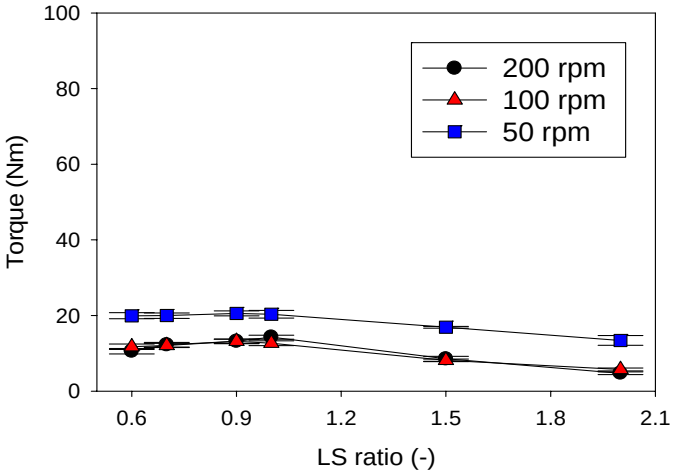

(b) PEG 6k 33%, dry powder feed rate: 10 g/min

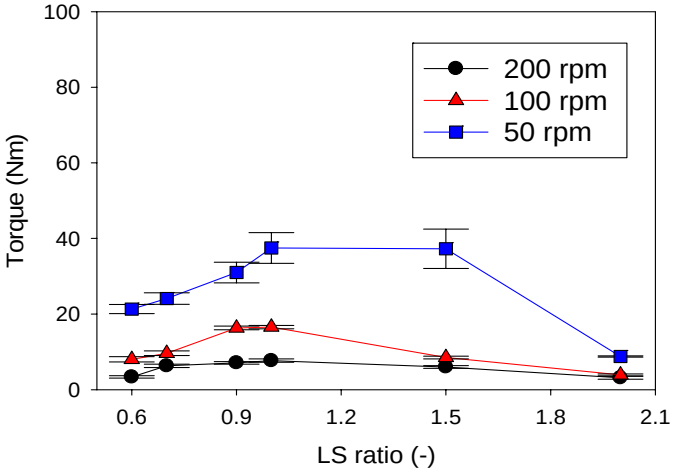

(c) Water, dry powder feed rate: 20 g/min

Fig. 4-4 Torque analyses

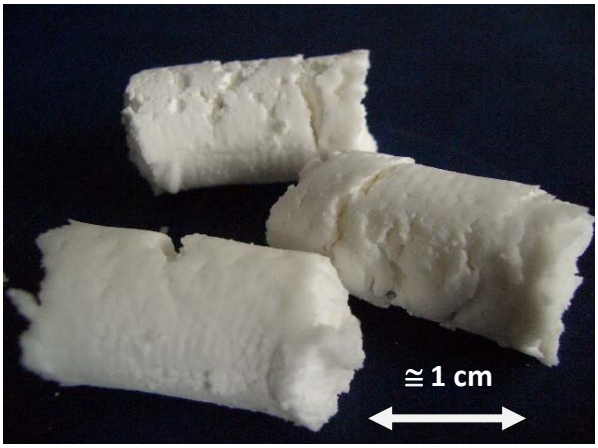

Fig. 4-5 The extrudates

4.4 Improving the GSD

Fig. 4-3 (b) indicates that a narrower GSD could be achieved with more binder addition and a faster rotating speed. However this conclusion was made based on a screw geometry featuring with a short and mild mixing section (16 mm, 30 degrees). It was still unclear that whether the length of mixing section (mixing time) or the mixing section geometry (aggressive mixing or mild mixing) could be the key factor to improve and narrow the GSD. Thus, two experiments for this question were made as below:

4.4.1 Looping experiment

Looping experiment is to put more work onto the granules by continuously reprocessing them under the same operating conditions. The granules were collected from the barrel exit and sampled. The rest of the granules were tipped back to the feeding hopper immediately for the next run. The binder addition will be stopped after finishing the first loop to remain the same LS ratio in the system. By repeating the looping procedure, the granules can be considered done with more work although it is not a typical continuous

process. The advantage of this attempting approach is that more work can be done without elongating the length of the barrel. Another method to put more work onto granules is to use any screw geometry (usually aggressive in mixing) that can lead to high torque. This can save the time that has been spent on looping. Note that the effects of different geometry would represent other dominating mechanisms and will be studied in Section 4.4.2.

Three experiments (experiments E07, E10 & E13) from the extruder working matrix - **Fig. 3-6** were chosen considering the suggestions from **Fig. 4-3 (b)**. 10 loops were processed and the samples were collected at the end of each loop. These samples were then dried out in an oven at 50˚C for 2 hrs before sieving. **Fig. 4-6** shows the GSD evolution in each condition. It is very clear that in the first loop of each condition, LS ratio has a strong effect on the GSD, which is in accordance with **Fig. 4-1**.

Regardless of the LS ratio, all the GSDs in **Fig. 4-6** were found to be more constant and uniform with time. **Fig. 4-7 (a)** compares the change of mean granule sizes of **Figs. 4-6 (a), (b)** and **(c)**. The mean granule size (d_{mgs}) was obtained by following eq. (4.2):

$$d_{mgs} = \sum_{i=1}^{n-1} \left(\frac{w_i \times d_i}{w_t}\right) \qquad (4.2)$$

where n is the number of sieves including a receiver ($sieve_{i=1}$), for which the aperture size is 0 μm. w_i is the weight of granules collected by $sieve_i$ and w_t is the total weight summed up from $sieve_{i=1}$ to $sieve_{i=n-1}$. d_i represents the mean diameter of the collecting sieve and the one above. The granules collected by the largest sieve ($sieve_{i=n}$) will be ignored in calculation, because the mean granule diameter of those granules is unknown.

It shows that the mean granule size is mainly dependent on the LS ratio for the first

loop, but this effect becomes less significant since the average sizes were down to a constant and tight range. It is interesting to compare this growth behaviour with the typical growth behaviour in high-shear granulation, where the mean granule size is usually increased from small towards big. When using an extruder to make granules, all the granules are produced via a processing barrel. It means that the granule growth will be constrained by the size of the barrel, and the final granule size cannot be larger than the screw channel. For a high-shear mixer granulator, the only geometric constraint on granules is the working vessel itself. Thus it allows a continuous size enlargement process until the granules are unable to sustain further impact forces.

The changes of each size frequency are displayed in **Figs. 4-7 (b), (c)** and **(d)** which are d_{16}, d_{50} and d_{84} respectively. These figures coincide with **Figs. 4-6** and **4-7 (a)** that the size distributions were very poor at the first loop, particularly at LS = 1.5 where many 'big and irregular shreds' (**Fig. 4-2**) were found.

The exerted work per unit mass was obtained by dividing the total work with the total mass as shown below, where W is work, F is force, s is displacement, r is radius, θ is radian and w is angular velocity. Thus the heat loss became zero and the effect of residence time can be ignored. Another simplification is to calculate it with average torque.

$$dW = Fds = Frd\theta = Torque \quad d\theta \tag{4.3 a}$$

$$\int dW = \int Torque \quad d\theta \tag{4.3 b}$$

$$W = Torque \times \theta = Torque \times \left(w \times \frac{2\pi}{60} \times time(\sec) \right) \tag{4.3 c}$$

$$\frac{Torque \times \left(w \times \frac{2\pi}{60} \times time(\sec) \right)}{Total \quad mass} \text{ (unit: kJ/g)} \tag{4.3 d}$$

Figs. 4-6 to **4-8** confirm that prolonging the processing time can achieve a uniform GSD regardless of the LS ratio. It suggests that a longer mixing time could be one option to improve the uniformity of GSD. It was noted that while **Fig. 4-8** showed that more work had been done at a lower LS ratio, no significant effect of the higher work was observed in respect of average granule size and GSD. One possible reason is that lack of binder resulted in higher torque so that the total work was consequently higher (see eq. (4.3 c)). More work done to the granules seemed to be an ideal method to achieve uniform GSD but it is unable to continuously increase the final granule size like high shear mixers due to the fixed barrel size. In addition, the work shown in **Fig. 4-8** was found increased loop by loop gradually. It was probably because the granules were dried out with the absence of air so that the comparison between the works done in each loop will not be the same.

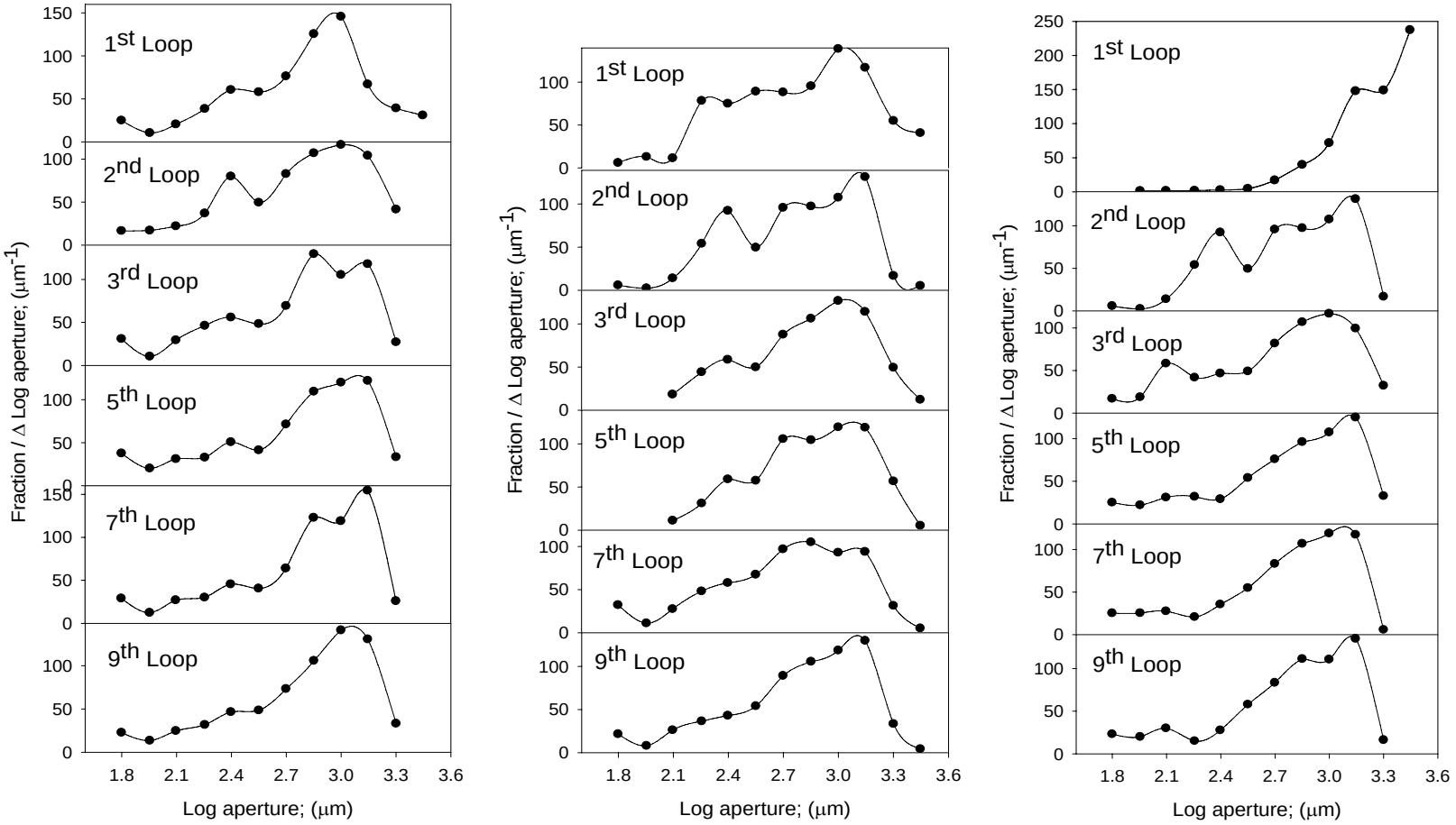

(a) LS = 0.9, 200 rpm **(b) LS = 1.0, 200 rpm** **(c) LS = 1.5, 200 rpm**

Fig. 4-6 Looping experiments

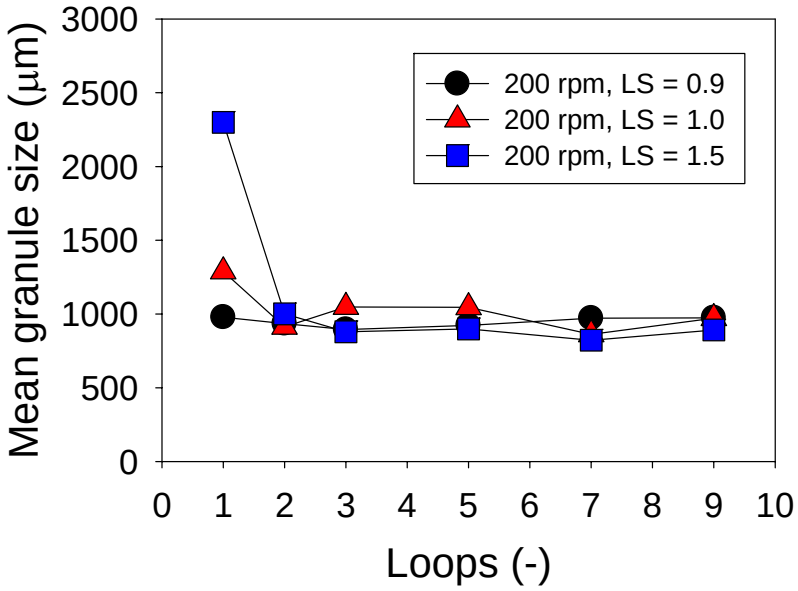

(a) The change of mean granule size

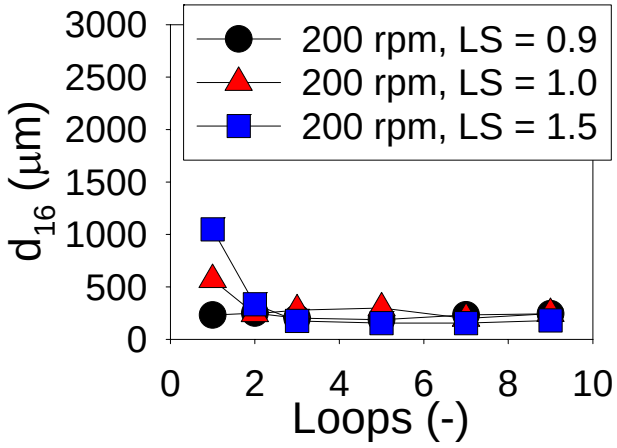

(b) The change of d_{16}

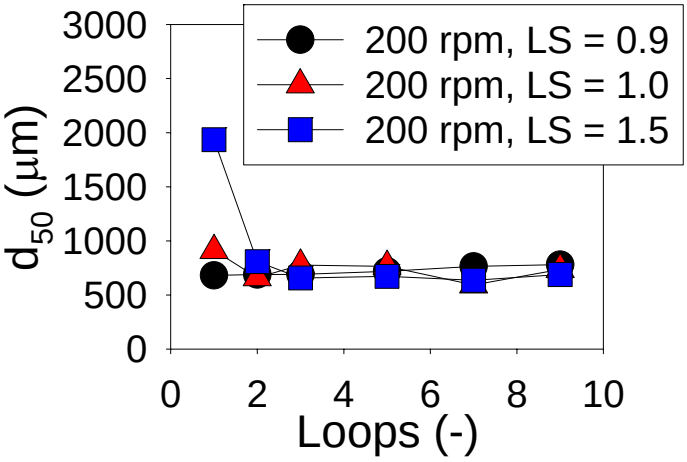

(c) The change of d_{50}

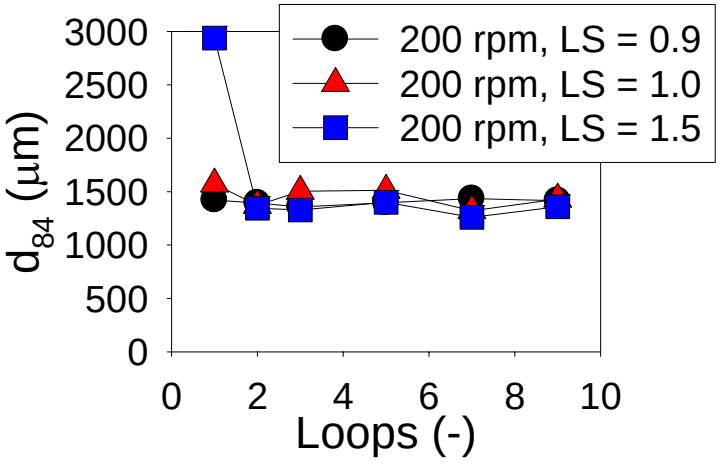

(d) The change of d_{84}

Fig. 4-7 The change of the mean granule size and each size frequency

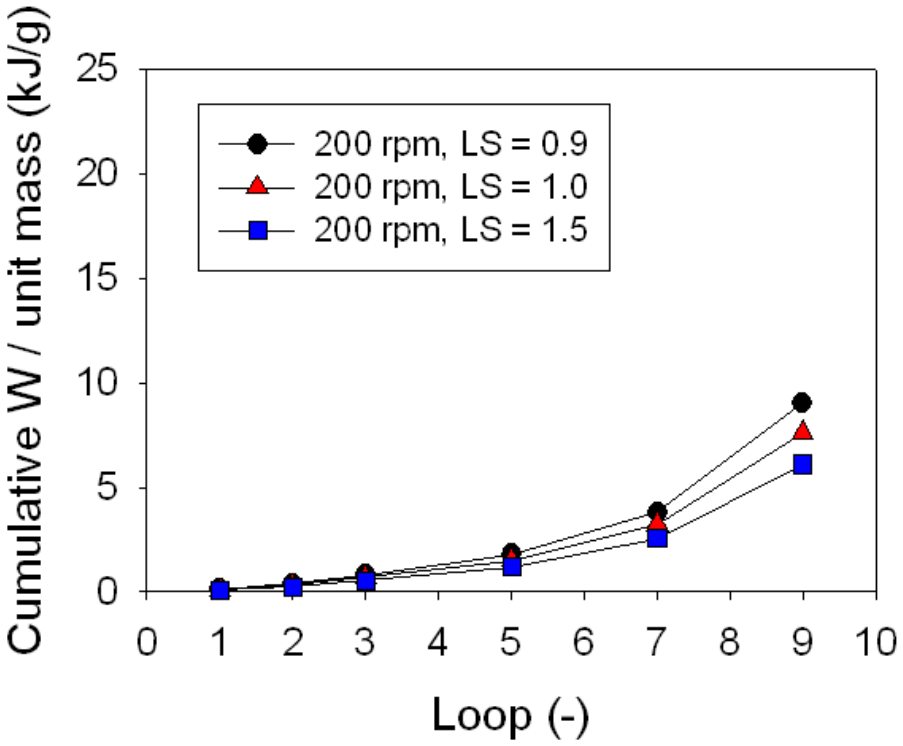

Fig. 4-8 The work exerted on the granules with the short single mixing section

4.4.2 Long single mixing section

Instead of the short single mixing section (16 mm and 30 degrees), a four times longer length of mixing section (64 mm and 30 degrees) was replaced. It was to reproduce looping effect by processing the mixture for longer time in a single pass. The operating conditions remained the same with Section 4.1.

As shown in **Fig. 4-9**, a longer mixing section resulted in a very different GSD across the matrix comparing to **Fig. 4-1** and formed another regime map. Generally, three main regimes in **Fig. 4-9** were recognised: granulation, extrudates and blocked regimes. For the regime of granulation, the GSD were still strongly dependent of LS ratio regardless of the screw speed. The peaks of the GSD were shifted from left to right with the increase of liquid addition. Also, higher screw speed was found helpful to narrow the GSD, because the big

and irregular shreds can be avoided. **Fig. 4-10** is the torque of granulation regime of this geometry. It is very similar to **Fig. 4-4 (a)** although the length of mixing section has been elongated to four times of the short one. This implies that high torque was caused by local jamming occurred within the barrel. The degree of local jamming can be increased by either low screw speed or high filling capacity. And when it exceeds a critical value, blocked regime may be observed.

In this thesis, the blocked regime was defined as followed: if the extruder encountered a high torque (>175 Nm), it will automatically shut down to protect the drive system and screws. This behaviour was found when the system was at 50 rpm, except for the over wetted state: LS = 2.0 where the mixture acted like a paste. When more liquid was added at the system of 50 rpm, the screws started rotating again and the system exhibited the extrudate behaviour because the over wetted materials cannot make granules but extrudates. If the screw speed in the extrudates behaviour was increased to 200 rpm (E13 in **Fig. 3-6**), granules were produced instead of extrudates. In high shear granulation, the effect of rotating speed remains minor until enough binder presents in the system. However when the twin screw extruder was at high LS (LS = 1.5 and 2.0), the effect of high speed on granule size was not as significant as high shear mixers and was only observed between experiments E14 & E13. It was presumably because the consolidation achieved by the twin screw extruder is less than the high shear mixer in which higher LS can be tolerated and may even be required, unless a very high fill level presents in the twin screw extruder so that the mixture can be better consolidated.

Hypothetically, when the materials are added into the barrel, they have to be conveyed through all the sections within the barrel. Take this research for example; the mixture has to

travel through a conveying section, mixing section, conveying section and finally a kneading section. Considering that the mixture is only rolled forward by the conveying section, a significant mixing can only occur in the mixing section. While the mixture stays in the mixing section, it will be slowly conveyed forward, thus the material can be accumulated and therefore mixed with the upcoming materials. Consequently, the local fill level will be increased, leading to a material consolidation stage, until the incoming mixture arrives and expels the consolidated mixture to the next section - kneading, a section that only provides consolidation.

Based on this hypothesis, the big and irregular shreds from 50 rpm & short single mixing section in **Fig. 4-1** were possibly caused by the over-consolidation (very high fill level). Sequentially, a high fill level can cause a high torque. This became more significant with a long single mixing section and therefore led the extruder being blocked (blocked regime in **Fig. 4-9**), until the screw speed was raised to 100 and 200 rpm.

As seen in **Fig. 4-10**, the torque in the longer-mixing-section extruder is obviously higher than the case of short single mixing section (**Fig. 4-4 (a)**). Although the length of the mixing section has been elongated by four times, the torque however was only about two times higher. This means the relationship between length of mixing section and torque is not linear and it will be worthy of further research on this relationship in the future. In addition, the effect of LS ratio on torque was the same with **Fig. 4-4 (a)** that binder addition can result in a higher torque until reaching a critical amount. And, high screw speed (low fill level) led to low torque due to insufficient friction forces.

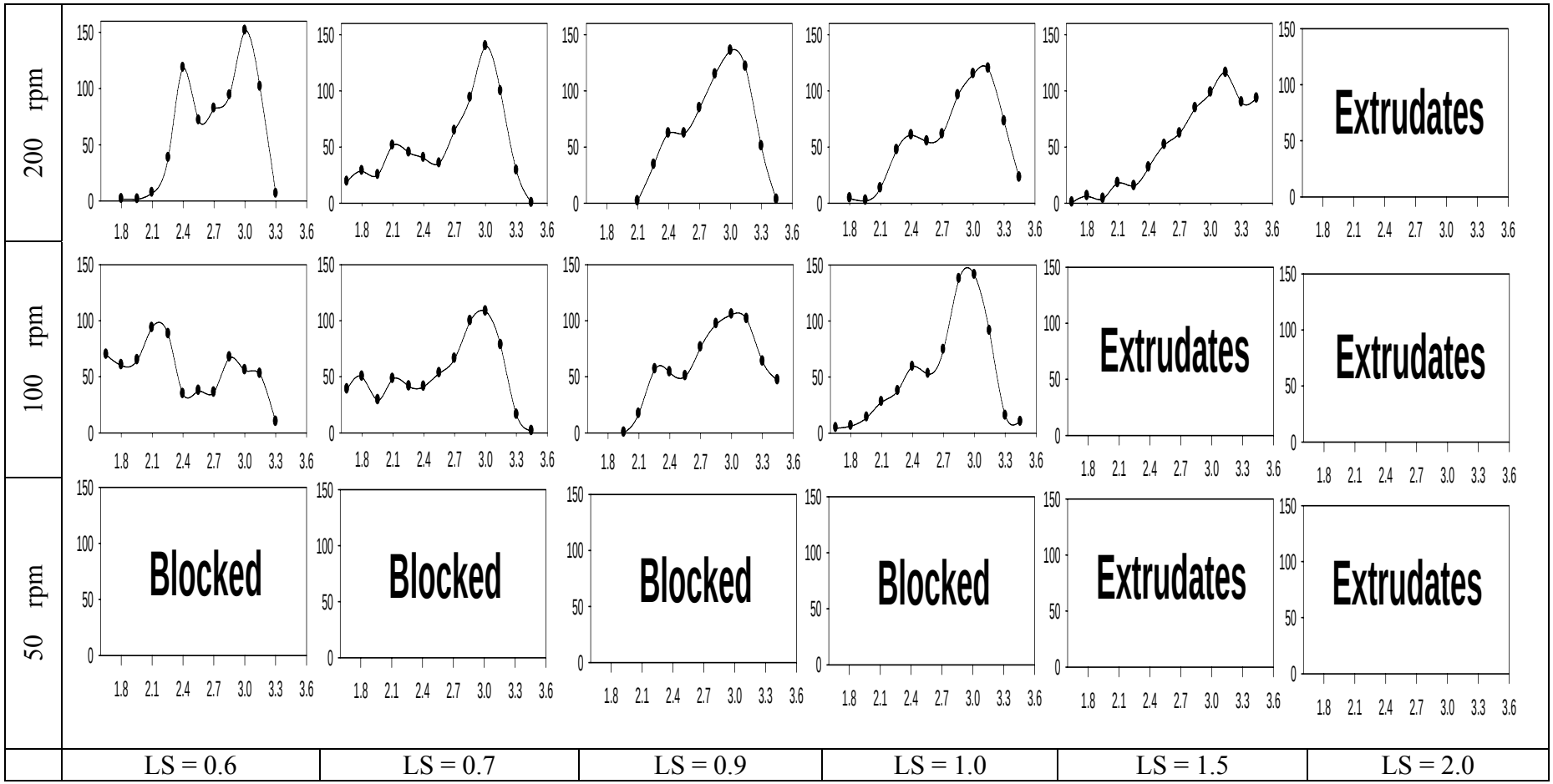

Fig. 4-9 The growth regime map for the extruder with a long single mixing section. Powder: MCC PH 102, Binder: aqueous PEG 6k 33%

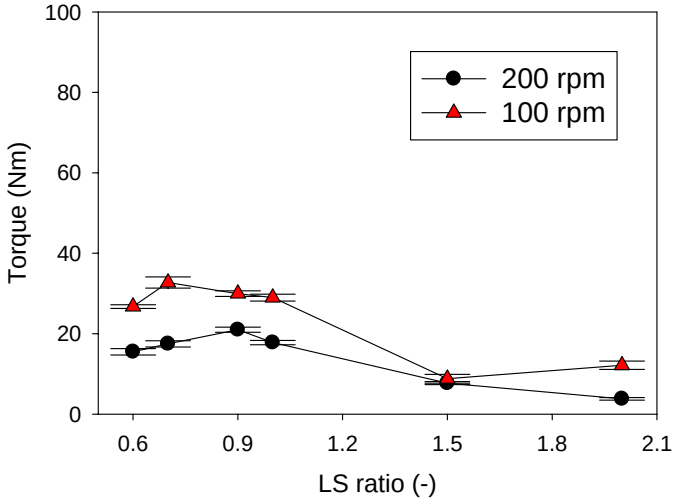

Fig. 4-10 Torque measurements with the long single mixing section. PEG 6k 33%, dry powder feed rate: 20 g/min

The GSDs in **Fig. 4-9** were further analysed as shown in **Figs. 4-11 (a)** and **4-11 (b).** Both figures show the same findings with the short single mixing section geometry: a big average granule size as well as a narrow GSD (small spread) can be achieved with a high screw speed (200 rpm) and a high LS ratio.

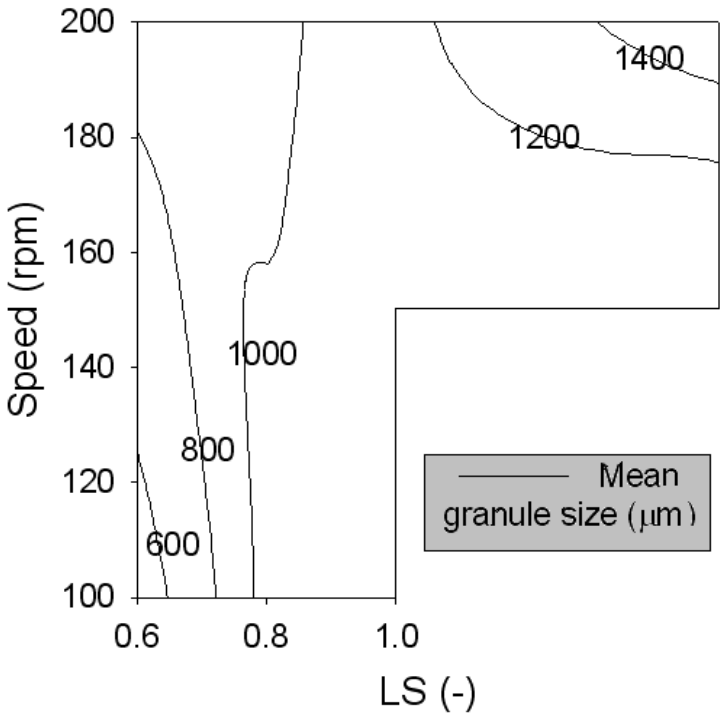

(a) Mean granule size

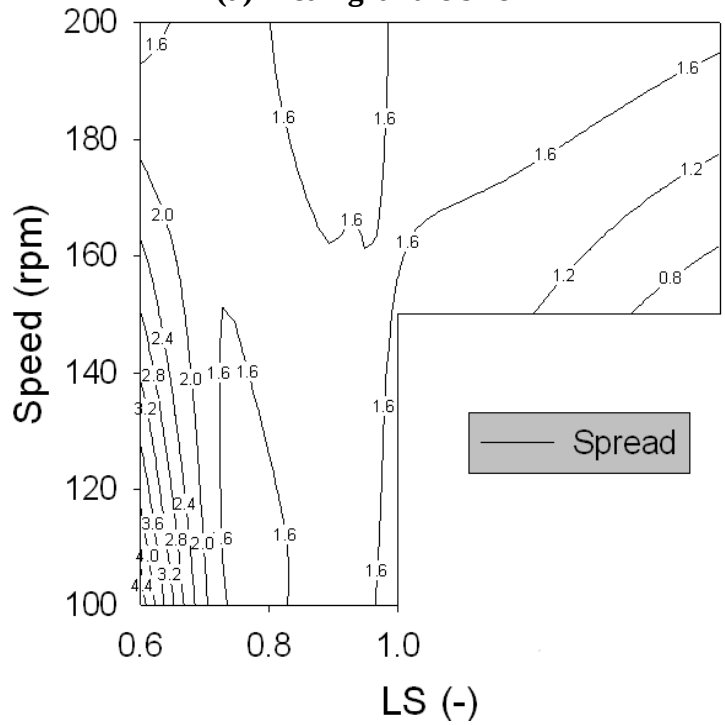

(b) Spread

Fig. 4-11 Further analysis of the GSD

A further comparison – looping experiment, was made to evaluate the effect of processing time on GSD. In order to compare the long-mixing-section extruder with **Fig. 4-6** on the same basis, the same operating conditions with **Fig. 4-6** were chosen (experiments E07, E10 and E13) and the GSD evolutions were shown in **Fig. 4-12**.

Generally for all the first loops, LS ratio did not play a very significant role to change the GSD uniformity. This was different from the LS effect in **Fig. 4-6**. It was because the mixing geometry in **Fig. 4-12** has become longer, presumably leading to a better binder distribution among granules, therefore the first-loop GSDs were similar to each other regardless of LS ratio. Homogeneous binder distribution in rotating drums [54] and high shear granulation [55] has been approved to be the key step to achieve uniform GSD. This thesis presumes that the same mechanism applies to the twin screw extruder granulation because it is true that longer mixing path should mix the solid and binder better than the shorter one. Future work regarding the relationship between mixing geometry and binder distribution amongst granules would be required to further understand the binder transportation between granules and the accompanying growth mechanisms. It is believed that due the same hypothetical assumption, all the GSDs shown in **Figs. 4-12 (a), (b) & (c)** have quickly become independent of LS and the processing time since the second loop. Although longer mixing path can provide a better mixing ability, the mass fraction of fines was found being increased when the looping experiments progressed because this geometry will also sequentially result in breakage.

Fig. 4-13 (a) shows the evolution of the mean granule size against different LS ratios. It can be seen that different LS ratios had a similar effect with the geometry of short single

mixing section as big granules were found with a high LS ratio at the first loop. It was also found that the overall size fluctuation in **Fig. 4-13 (a)** was less than **Fig. 4-7 (a)**, including d_{16}, d_{50} and d_{84} as shown in **Figs. 4-13 (b), (c)** and **(d)**. Again this could be contributed by better mixing of solids and binder which is the result of the longer mixing path.

Up to this Section, the operating conditions for obtaining uniform GSD are recommended here: a system with higher screw speed, a higher LS ratio and a better mixing (either a longer processing time or an aggressive mixing geometry).

The total work done per unit mass was calculated by following equations (4.3 a) to (4.3 d) and plotted in **Fig. 4-14**. It shows the same effect of LS ratio with what has been seen in **Fig. 4-8** but the amount of work are greater due to the higher torque.

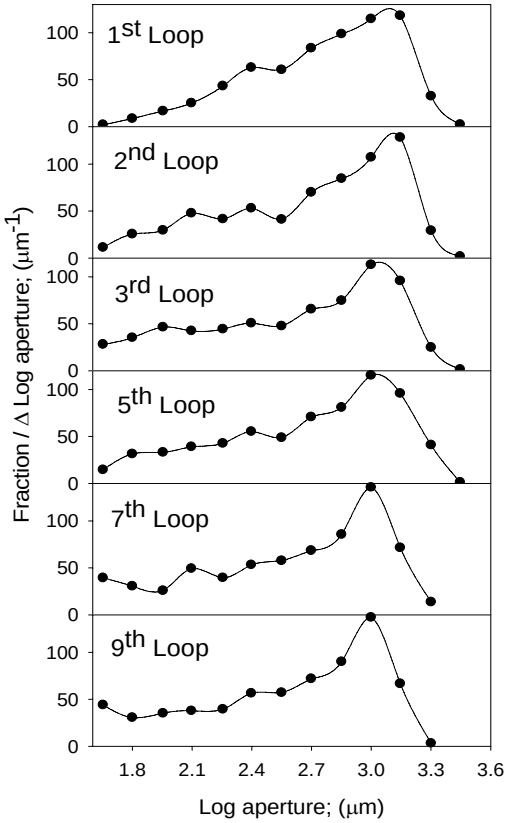

(a) LS = 0.9, 200 rpm

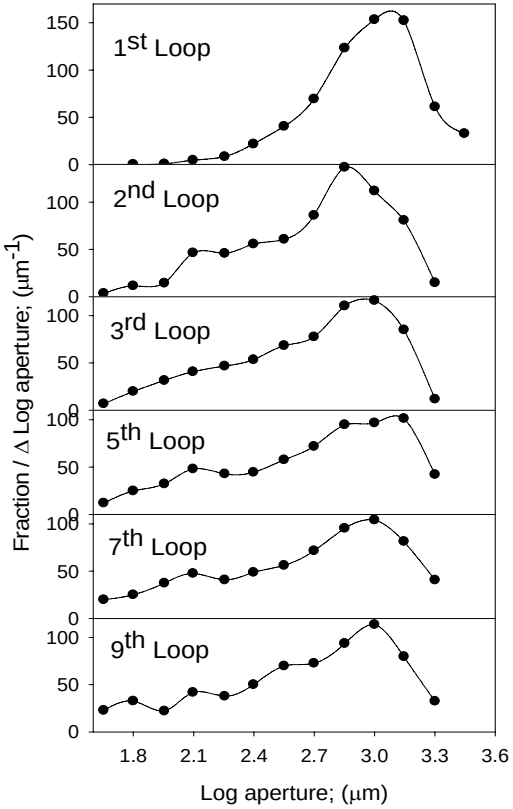

(b) LS = 1.0, 200 rpm

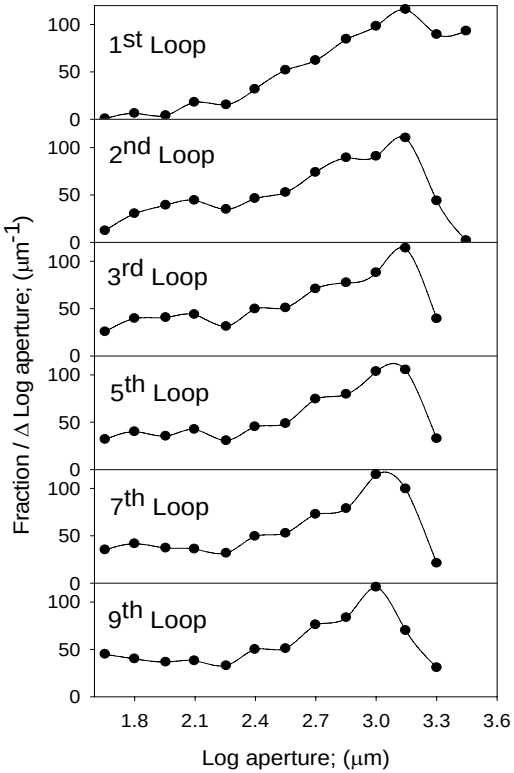

(c) LS = 1.5, 200 rpm

Fig. 4-12 Looping experiments

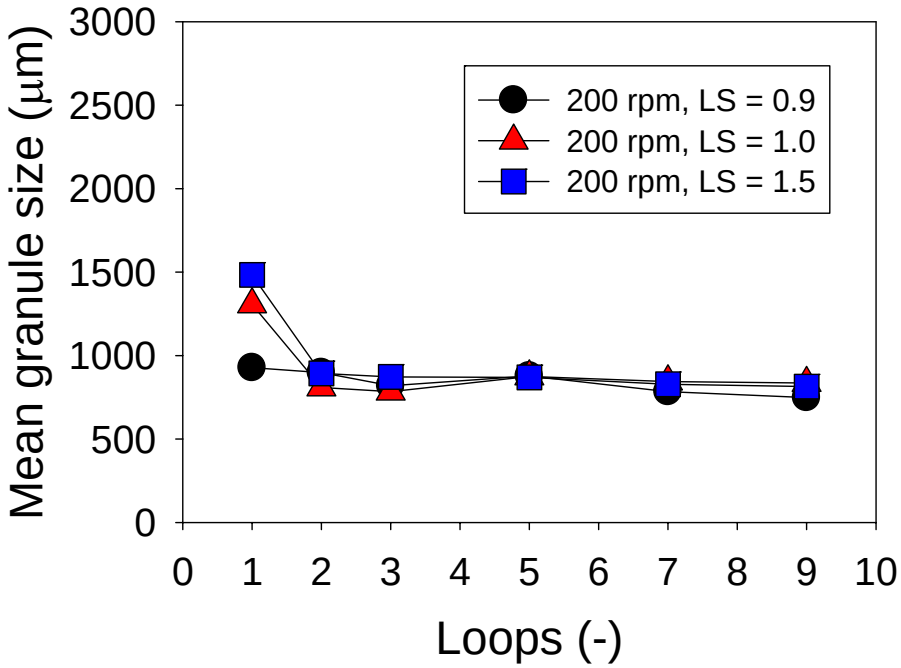

(a) The change of mean granule size

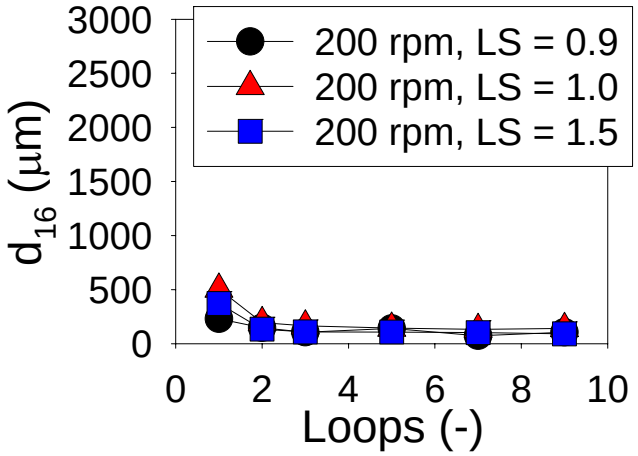

(b) The change of d_{16}

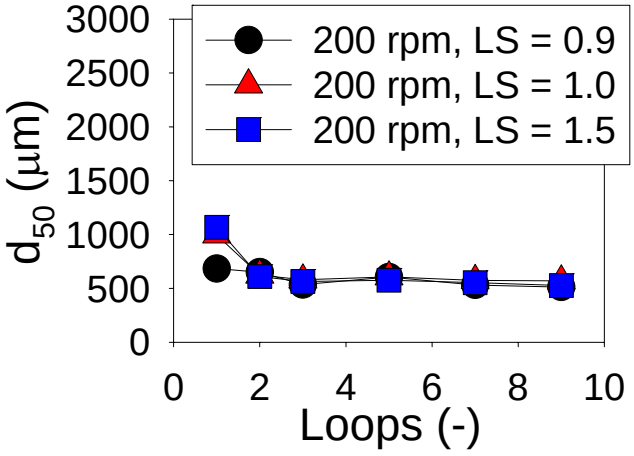

(c) The change of d_{50}

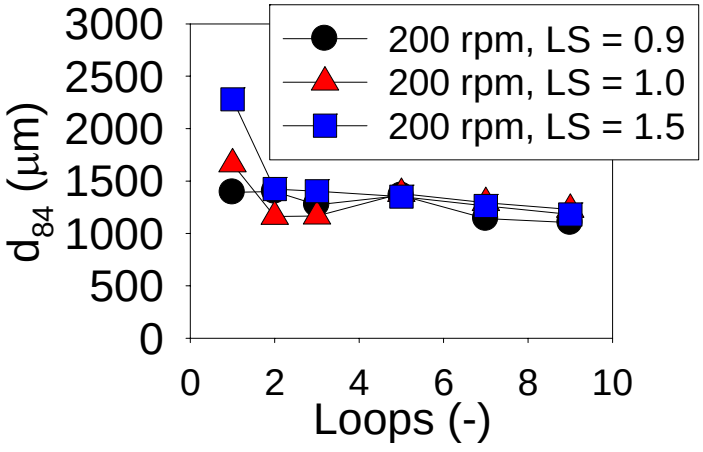

(d) The change of d_{84}

Fig. 4-13 The change of the mean granule size and each size frequency

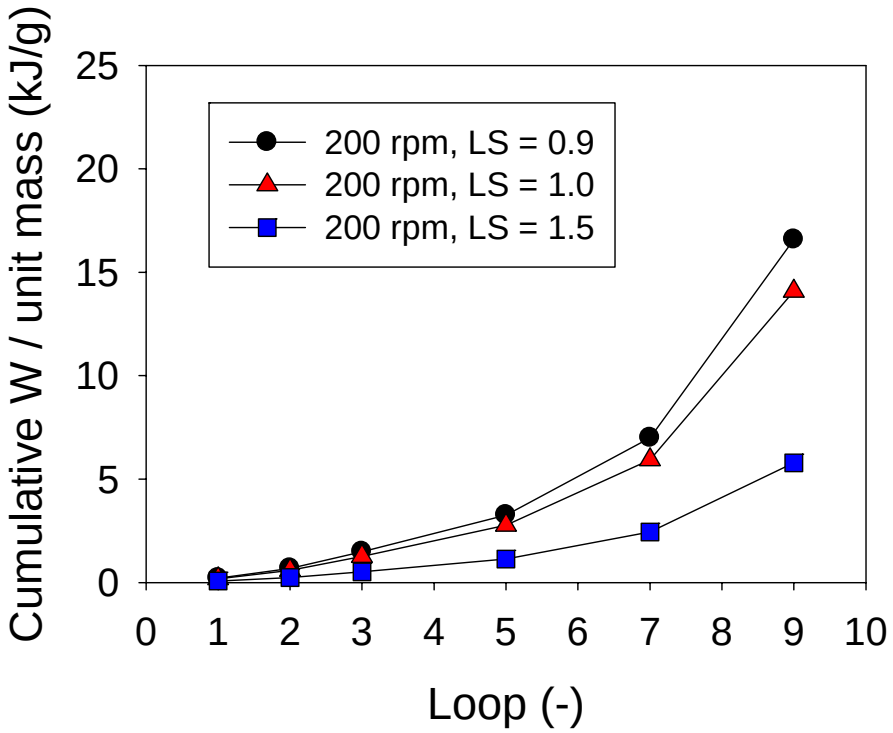

Fig. 4-14 The work exerted on the granules with a long single mixing section

4.4.3 Staggered mixing sections

There are two reasons for this new configuration. First of all, this Section is to further investigate the characteristics of a more complicated and commonly seen screw geometry, based on the results obtained in Sections 4.4.1 & 4.4.2. Secondly, one of the main conclusions from Section 4.4.2 is that better mixing could the key factor to effectively improve the uniformity of GSD; however, the detail of mixing process within the mixing zone remains a challenge to understand. Therefore this Section aims to find out whether the time dependent mixing zones exist, and this could be the key step prior to elucidating the effects of extended mixing path.

The so called staggered mixing geometry is to separate the mixing geometry that has been used in Section 4.4.2 into two equal parts and installed them just downstream of the first and second liquid injection ports shown in **Fig. 3-8**. The rest of the geometry and

binder addition setup remained the same to keep the consistency throughout the thesis. **Fig. 4-15** shows the GSDs of each operating conditions across the working matrix. Three regimes were recognised– the granulation regime, the extrudate regime and the blocked regime. Interestingly, it was found that the same length of mixing path but with different arrangement can result in different GSDs as well as the regime map. It is the direct evidence that the mechanisms of extruder granulation can be changed by simply rearranging original mixing elements.

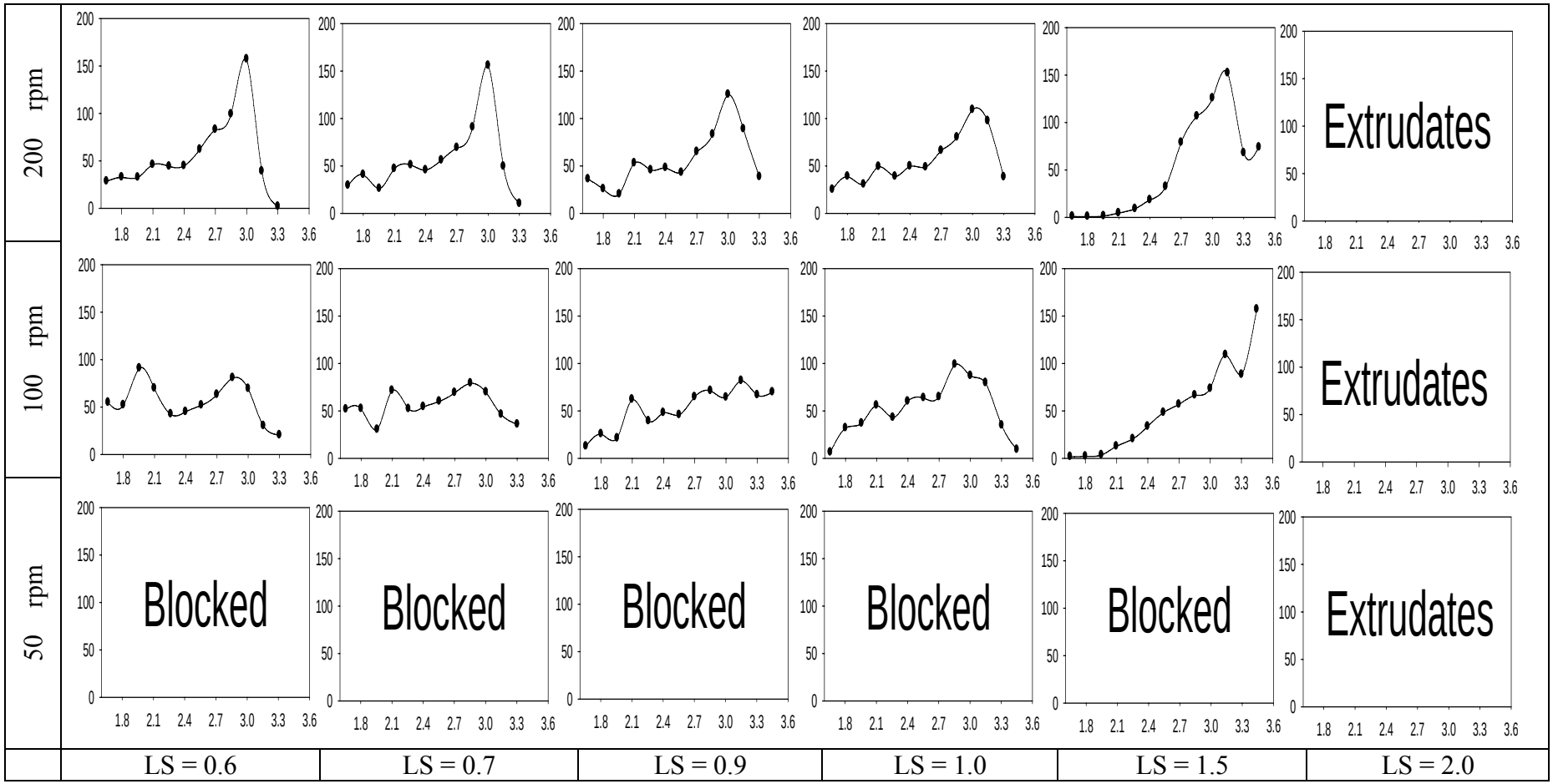

Fig. 4-15 The growth regime map for the extruder with staggered mixing sections. Powder: MCC PH 102, Binder: aqueous PEG 6k 33%

As shown in **Figs 4-16 (a)** & **(b)**, the conditions for producing large granules with narrow GSD are high rotating speed and more binder addition and these coincide with the conclusions obtained in Sections 4.4.1 and 4.4.2. Interestingly, high shear granulation requires the same conditions – while sufficient binder addition is a requirement for granule growth there is an equally important requirement for distribution of this binder and that low impeller speeds impart insufficient energy to achieve this. According to the proposing mechanisms made in Section 4.4.1 and 4.4.2 that sufficient mixing could be the key factor to achieve large granules with narrow GSD, the staggered mixing sections seem not be able to provide better mixing than the long single mixing zone (used in Section 4.4.2). As an imaginary plot shown in **Fig. 4-17**, the amount of mixing could be a function of the length of the mixing path, however, the mixing index goes gradually into a plateau, because the degree of mixing of powders and binder should theoretically go towards 1 for a "fully mixed state."

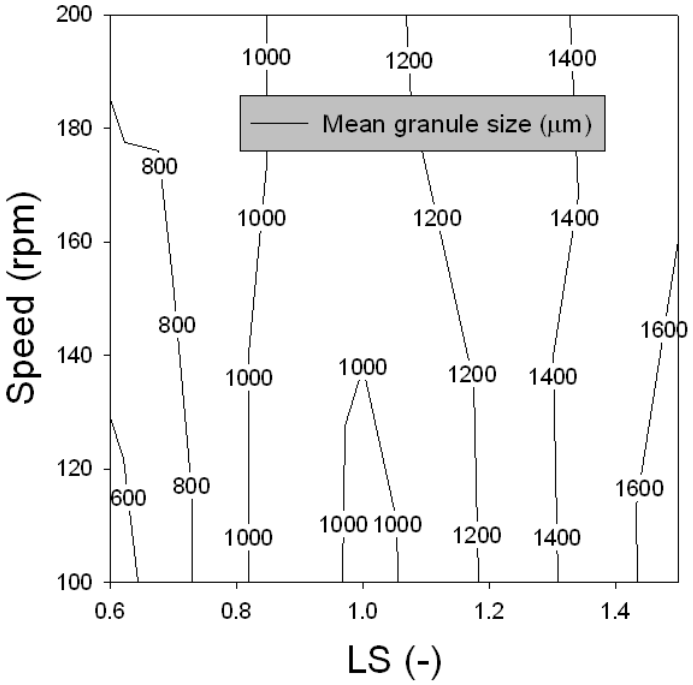

(a) Mean granule size

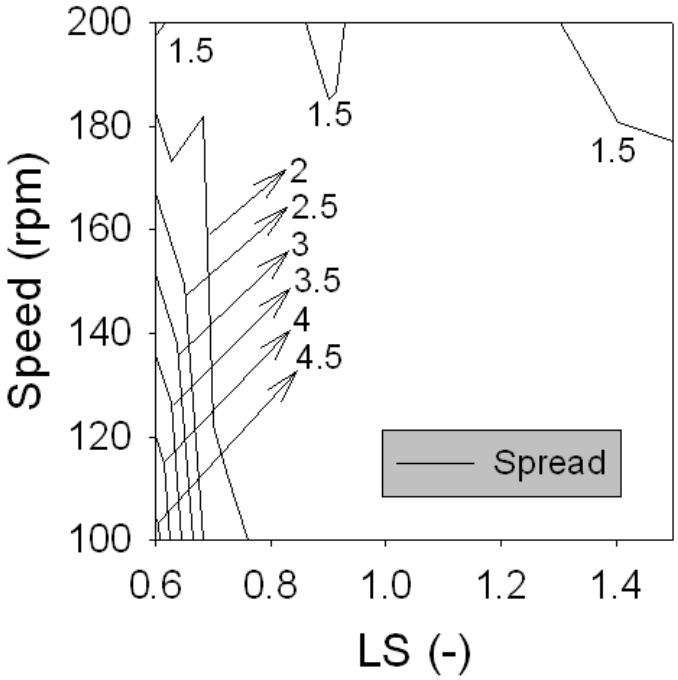

(b) Spread

Fig. 4-16 Further analysis of the GSD

Another interesting finding was that the area of extrudate regime in **Fig. 4-15** is smaller than that in **Fig. 4-9** because the experiment E14 has become a part of the granulation regime and E15 has become a part of the blocked regime. Following the proposing mechanisms made in Section 4.4.2 that the higher "consolidation rate" applied on mixtures, the paste (extrudate regime) is more likely to become granules. This geometry (staggered mixing section) suggested that the "amount of consolidation" is also one possible factor. As shown in **Fig. 4-17**, the consolidation index goes up linearly until the end of a mixing zone because the longer the consolidation time, the mixture should be harder regardless of the consolidation rate. Therefore it was observed that the longer mixing path (long single mixing section and staggered mixing section) tends to enable the blocked regimes. To approve the feasibility of **Fig. 4-17**, it is suggested to investigate the texture of paste along with barrel in the future and the detail will be discussed in Chapter 6.

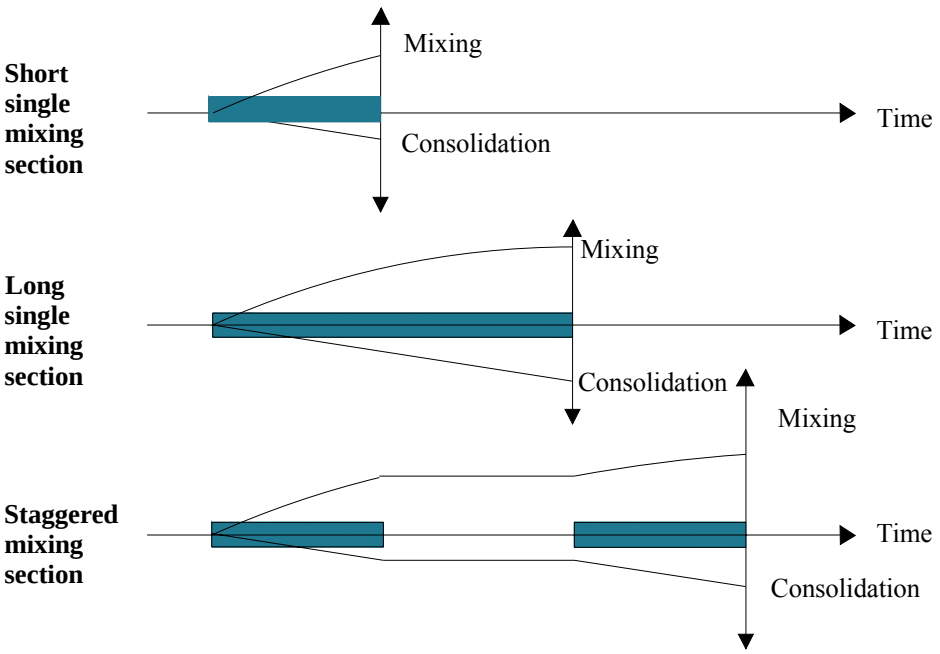

Fig. 4-17 Comparisons between short, long single mixing section and staggered mixing section

CHAPTER FIVE
CONCLUSIONS AND COMMENTS

This thesis demonstrates the effects of screw speed, LS ratio and screw geometry on twin screw extruder granulation. Regime maps for the systems are drawn and the specific behaviours are recognised. The maps as well as the underlying mechanisms are then compared with the one developed in high-shear wet granulation.

Comparing to a typical high-shear wet granulation, the effect of extruder screw speed is mainly to change the fill level in the barrel. With a higher fill level in the barrel, higher friction force as well as higher torque can be observed. Besides, the effect of LS ratio in extruder granulation is to change the friction force between the mixture and the inner wall of the barrel. Increasing LS ratio will lead to a high fill level and the torque can be increased sequentially. After reaching a critical liquid amount, the mixture will become over-wetted and the torque will become low.

By measuring the GSD of final products, this work develops three extruder granulation regime maps for the short-single, long-single and staggered mixing geometries. For the short-single one, a granulation regime and a extrudate regime are recognised; for the long-single one, three regimes are recognized: granulation, extrudates and the blocked regimes; for the staggered geometry, three regimes are recognized: granulation, extrudates

and the blocked regimes, but the layout is different from the long-single one.

Overall, the granules with big size and a narrow GSD can be achieved with more binder addition, higher screw speed and any geometry that can provide sufficient mixing. And these coincide with high shear wet granulation - while sufficient binder addition is a requirement for granule growth there is an equally important requirement for distribution of this binder and that low impeller speeds impart insufficient energy to achieve this.

This thesis also proposes hypothetical mechanisms for the extruder granulation: the mixing only occurs within the mixing zones and the degree of it will approach 1 gradually. On the other hand, the degree of consolidation is a function of the mixing path, so that the longer mixing zones are more likely to transform paste into granulation or even the blocked regime.

CHAPTER SIX
FUTURE WORKS

In order to develop systematic and new regime maps for extruder granulation this thesis employs the idea from high-shear wet granulation, although some practical challenges were found:

1. How to measure the time dependent properties precisely?

   Sampling granules and the upcoming analysis determine a typical growth regime map in high shear wet granulation. The material exchange can be figured by tracking the changes of each size frequency. Unlike to common granulation processes (drum, high shear granulator or Wurster coater etc.) where granules are exposed to the air, sampling in an extruder is not easy because: (1) the interior space of the barrel is tightly enclosed, resulting in a highly mass flux across the channel; (2) furthermore, the material flows with an unknown velocity profile within the barrel. Therefore it is difficult to collect 'representative granules' at one fixed port.

   An attempted approach called 'freezing method' has been tried by stopping the process while running. Open the barrel and collect the granules afterwards immediately. However it failed because the granules were spilled out everywhere and sometimes the other materials were found jammed at mixing sections (hypothetically considered "consolidation stage") as shown in **Fig. 6-1**.

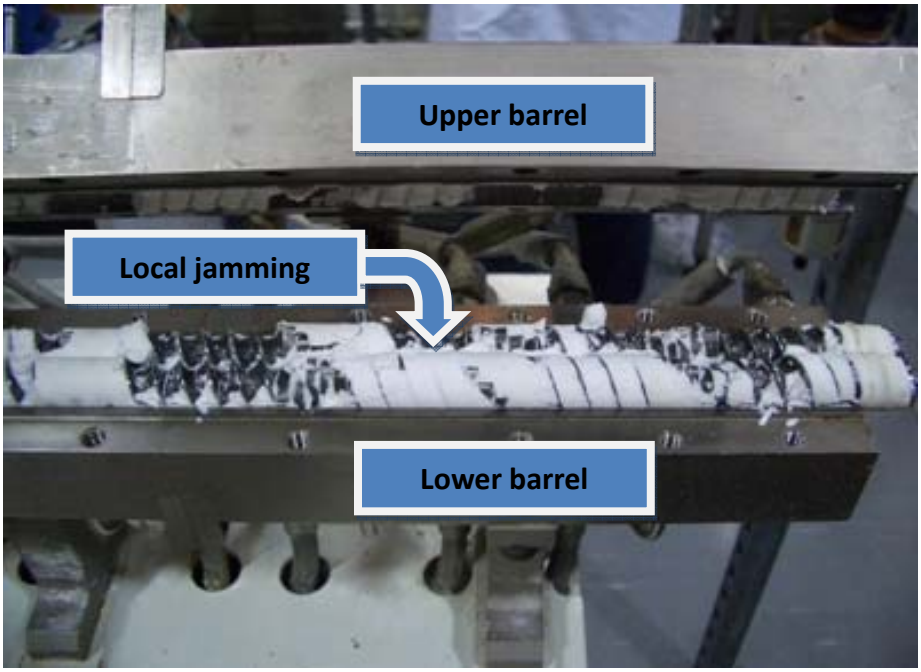

Fig. 6-1 The Freezing method

A proper sampling apparatus would be required in this case to collect "representative granules" by not suspending the granulation processes. Therefore the measurement of time dependant properties within the mixing sections, such as mixing index, density gradient, hardness etc could become feasible and this is the vital step to understand the transportation phenomena.

2. What are the effects of other geometries?

The geometries in this thesis are set to be simpler than the ones in practice, aiming to ease the complexity of flow pattern. Thus the proposed granulation behaviours according to these geometries are sure to be at a fundamental stage. It is still a lack of direct relationships between simple geometries to reality.

Comprehensively understanding the effects of different mixing sections (aggressive or multi sections) is important for regime map development as well as investigating the formulation mechanisms. Some experiments are suggested: (1) Different separated distance between mixing sections. It helps explain how the staggered distance affect the granulation mechanisms; (2) Measurement of the mixing mechanism. There are two mixing mechanisms in polymer extrusion which are the distributive mixing and dispersive mixing mechanisms, respectively. It has been known that distributive mixing must occur in this thesis because the liquid phase is distributed amongst the solid phase. We could also assume dispersive mixing occurs at some extent because it is usually observed in these systems. These measurements would be suggested as it can characterize the governing mixing mechanisms.

3. Energy consumption monitoring

In industry, total energy consumption is used to be simple and direct information to monitor the manufacturing processes. However this thesis simplified the calculation by ignoring the effects of "residence time distribution", a very common measurement found in the literatures of twin screw extrusion. This experimental work will be suggested to take into account nevertheless. Besides, via the residence time distribution measurement, the binder distribution among granules and extrudates could also be understood.

It is practically difficult to collect granules as well as visualizing the real flow pattern during the process; therefore this thesis can only propose a hypothesis of

extruder granulation based on the granule morphology and draw the regime maps accordingly. With the suggested experimental plans mentioned above, a better understanding of extruder granulation can be achieved and a full extent of granulation mechanisms can be defined.

Reference List

[1] W. D. Tu, A. Ingram, J. P. K. Seville, and S. S. Hsiau, Exploring the regime map for high-shear mixer granulation, Chemical Engineering Journal, 145 (2009) 505-513.

[2] M. Rhodes, Introduction to Particle Technology, John Wiley & Sons, 1998.

[3] A. S. Blair, Dust explosion incidents and regulations in the United States, Journal of Loss Prevention in the Process Industries, 20 (2007) 523-529.

[4] K. Szymocha, Industrial applications of the agglomeration process, Powder Technology, 130 (2003) 462-467.

[5] D. Rossetti and S. J. R. Simons, A microscale investigation of liquid bridges in the spherical agglomeration process, Powder Technology, 130 (2003) 49-55.

[6] W. Pietsch, Agglomeration processes: phenomena, technologies, equipment, Wiley-VCH, 2002.

[7] K. L. Kadam, Granulation Technology for Bioproducts, Informa Health Care, Boston 1990.

[8] Granulation, Elsevier, Amsterdam 2007.

[9] M. Jacob, Granulation equipment, in: A. D. Salman, M. J. Hounslow, and J. P. K. Seville (Eds.), Granulation, Elsevier, Amsterdam, 2007, pp. 417-476.

[10] http://www.glatt.com/e/01_technologien/01_03_02_02.htm

[11] S. M. Iveson, J. D. Litster, K. Hapgood, and B. J. Ennis, Nucleation, growth and breakage phenomena in agitated wet granulation processes: a review, Powder Technology, 117 (2001) 3-39.

[12] S. M. Iveson, J. A. Beathe, and N. W. Page, The dynamic strength of partially saturated powder compacts: the effect of liquid properties, Powder Technology, 127 (2002) 149-161.

[13] T. Schaefer and C. Mathiesen, Melt pelletization in a high shear mixer. IX. Effects of binder particle size, International Journal of Pharmaceutics, 139 (1996) 139-148.

[14] S. M. Iveson, J. D. Litster, and B. J. Ennis, Fundamental studies of granule consolidation Part 1: Effects of binder content and binder viscosity, Powder Technology, 88 (1996) 15-20.

[15] J. S. Fu, Y. S. Cheong, G. K. Reynolds, M. J. Adams, A. D. Salman, and M. J. Hounslow, An experimental study of the variability in the properties and quality of wet granules, Powder Technology, 140 (2004) 209-216.

[16] G. I. Tardos, M. I. Khan, and P. R. Mort, Critical parameters and limiting conditions in binder granulation of fine powders, Powder Technology, 94 (1997) 245-258.

[17] S. M. Iveson, P. A. L. Wauters, S. Forrest, J. D. Litster, G. M. H. Meesters, and B. Scarlett, Growth regime map for liquid-bound granules: further development and experimental validation, Powder Technology, 117 (2001) 83-97.

[18] K. van den Dries, O. M. de Vegt, V. Girard, and H. Vromans, Granule breakage phenomena in a high shear mixer; influence of process and formulation variables and consequences on granule homogeneity, Powder Technology, 133 (2003) 228-236.

[19] P. C. Knight, J. P. K. Seville, A. B. Wellm, and T. Instone, Prediction of impeller torque in high shear powder mixers, Chemical Engineering Science, 56 (2001) 4457-4471.

[20] K. P. Hapgood, S. M. Iveson, J. D. Litster, and L. X. Liu, Granulation rate processes, in: A. D. Salman, M. J. Hounslow, and J. P. K. Seville (Eds.), Granulation, Elsevier, Amsterdam, 2007, pp. 897-978.

[21] S. M. Iveson and J. D. Litster, Growth regime map for liquid-bound granules, AIChE Journal, 44 (1998) 1510-1518.

[22] K. P. Hapgood, J. D. Litster, S. R. Biggs, and T. Howes, Drop penetration into porous powder beds, Journal of Colloid and Interface Science, 253 (2002) 353-366.

[23] S. L. Rough, D. I. Wilson, and D. W. York, A regime map for stages in high shear mixer agglomeration using ultra-high viscosity binders, Advanced Powder Technology, 16 (2005) 373-386.

[24] A. M. Bouwman, M. R. Visser, G. M. H. Meesters, and H. W. Frijlink, The use of Stokes deformation number as a predictive tool for material exchange behaviour of granules in the 'equilibrium phase' in high shear granulation, International Journal of Pharmaceutics, 318 (2006) 78-85.

[25] B. J. Ennis, G. Tardos, and R. Pfeffer, A microlevel-based characterization of granulation phenomena, Powder Technology, 65 (1991) 257-272.

[26] S. T. Keningley, P. C. Knight, and A. D. Marson, An investigation into the effects of binder viscosity on agglomeration behaviour, Powder Technology, 91 (1997) 95-103.

[27] B. J. Ennis, J. Li, G. I. Tardos, and R. Pfeffer, The influence of viscosity on the strength of an axially strained pendular liquid bridge, Chemical Engineering Science, 45 (1990) 3071-3088.

[28] G. Barnocky and R. H. Davis, Elastohydrodynamic collision and rebound of spheres: experimental verification, Physics of Fluids, 31 (1988) 1324-1329.

[29] I. Talu, G. I. Tardos, and M. I. Khan, Computer simulation of wet granulation, Powder Technology, 110 (2000) 59-75.

[30] P. J. T. Mills, J. P. K. Seville, P. C. Knight, and M. J. Adams, The effect of binder viscosity on particle agglomeration in a low shear mixer/agglomerator, Powder Technology, 113 (2000) 140-147.

[31] P. A. L. Wauters, R. van de Water, J. D. Litster, G. M. H. Meesters, and B. Scarlett, Growth and compaction behaviour of copper concentrate granules in a rotating drum, Powder Technology, 124 (2002) 230-237.

[32] F. Hoornaert, P. A. L. Wauters, G. M. H. Meesters, S. E. Pratsinis, and B. Scarlett, Agglomeration behaviour of powders in a Lodige mixer granulator, Powder Technology, 96 (1998) 116-128.

[33] P. C. Kapur, Balling and Granulation, Advances in Chemical Engineering, 10 (1978) 55-123.

[34] http://www.unitec-solution.de/e/01_technologien/01_04_03.htm

[35] H. Leuenberger, New trends in the production of pharmaceutical granules: batch versus continuous processing, European Journal of Pharmaceutics and Biopharmaceutics, 52 (2001) 289-296.

[36] E. I. Keleb, A. Vermeire, C. Vervaet, and J. P. Remon, Twin screw granulation as a simple and efficient tool for continuous wet granulation, International Journal of Pharmaceutics, 273 (2004) 183-194.

[37] E. I. Keleb, A. Vermeire, C. Vervaet, and J. P. Remon, Continuous twin screw extrusion for the wet granulation of lactose, International Journal of Pharmaceutics, 239 (2002) 69-80.

[38] M. Weinmann, Masterbatch production on co-rotating twin screw extruders, Plastics, Additives and Compounding, 9 (2007) 36-39.

[39] G. M. Owolabi, M. N. Bassim, J. H. Page, and M. G. Scanlon, The influence of specific mechanical energy on the ultrasonic characteristics of extruded dough, Journal of Food Engineering, 86 (2008) 202-206.

[40] M. J. Gamlen and C. Eardley, Continuous extrusion using a Baker Perkins MP50 (Multipurpose) extruder, Drug Development and Industrial Pharmacy, 12 (1986) 1701-1713.

[41] N. O. Lindberg, C. Tufvesson, and L. Olbjer, Extrusion of an effervescent granulation with twin extruder Baker Perkins MPF 50 D, Drug Development and Industrial Pharmacy, 13 (1987) 1891-1913.

[42] N. O. Lindberg, C. Tufvesson, P. Holm, and L. Olbjer, Extrusion of an effervescent granulation with twin screw extruder, Baker Perkins MPF 50 D. Influence on intra-granular porosity and liquid saturation, Drug Development and Industrial

Pharmacy, 14 (1988) 1791-1798.

[43] P. Kleinebudde and H. Lindner, Experiments with an instrumented twin-screw extruder using a single-step granulation/extrusion process, International Journal of Pharmaceutics, 94 (1993) 49-58.

[44] B. Van Melkebeke, B. Vermeulen, C. Vervaet, and J. P. Remon, Melt granulation using a twin-screw extruder: A case study, International Journal of Pharmaceutics, 326 (2006) 89-93.

[45] K. Nakamichi, T. Nakano, H. Yasuura, S. Izumi, and Y. Kawashima, Stabilization of sodium guaiazulene sulfonate in granules for tableting prepared using a twin-screw extruder, European Journal of Pharmaceutics and Biopharmaceutics, 56 (2003) 347-354.

[46] C. Schmidt and P. Kleinebudde, Comparison between a twin-screw extruder and a rotary ring die press. Part II: influence of process variables, European Journal of Pharmaceutics and Biopharmaceutics, 45 (1998) 173-179.

[47] E. I. Keleb, A. Vermeire, C. Vervaet, and J. P. Remon, Cold extrusion as a continuous single-step granulation and tabletting process, European Journal of Pharmaceutics and Biopharmaceutics, 52 (2001) 359-368.

[48] A. Darelius, A. Rasmuson, I. N. Bjö n, and S. Folestad, High shear wet granulation modelling-a mechanistic approach using population balances, Powder Technology, 160 (2005) 209-218.

[49] A. Kumar, G. M. Ganjyal, D. D. Jones, and M. A. Hanna, Digital image processing for measurement of residence time distribution in a laboratory extruder, Journal of Food Engineering, 75 (2006) 237-244.

[50] C. Bi, B. Jiang, and A. Li, Digital image processing method for measuring the residence time distribution in a plasticating extruder, Polymer Engineering & Science, 47 (2007) 1108-1113.

[51] K. Eise, H. Herrmann, S. Jakopin, U. Burkhardt, and H. Werner, An analysis of twin-screw extruder mechanisms, Advances in Polymer Technology, 1 (1981) 18-39.

[52] N. P. Cheremisinoff, Composites and specialty application, Handbook of Polymer Science and Technology, CRC Press, 1989.

[53] Pharmaceutical Dosage Forms: Tablets, Informa Health Care, 1989.

[54] P. C. Knight, T. Instone, J. M. K. Pearson, and M. J. Hounslow, An investigation into the kinetics of liquid distribution and growth in high shear mixer agglomeration, Powder Technology, 97 (1998) 246-257.

[55] W. D. Tu, S. S. Hsiau, A. Ingram, and J. Seville, The effect of powder size on induction behaviour and binder distribution during high shear melt agglomeration of calcium carbonate, Powder Technology, 184 (2008) 298-312.